Progress of Theoretical Physics, Vol. 40, No. 6, December 1968

Theory of Spin-Wave Impurity States in an Antiferromagnet

Takashi TONEGAWA*)

Department of Physics, Faculty of Science
Osaka University, Toyonaka, Osaka

(Received May 31, 1968)

The effect of a single substituted impurity spin on the spin-wave spectrum of an insulating antiferromagnet is investigated. The linear spin-wave theory of the impurity state is developed for a spin Hamiltonian including an intersublattice Heisenberg exchange term and an anisotropy energy term of the form, $-DS_z^2$. Green's function techniques are used. Both the cases of a ferromagnetically and antiferromagnetically coupled impurity spin are studied. In the numerical calculations we confine ourselves to the body-centered cubic and MnF_2 (rutile)-type lattices, which are topologically equivalent to each other in the present Hamiltonian. Numerical results both of the conditions under which the *s*, *p*, *d* and *f* type localized modes appear and of the energies of these localized modes are presented for various combinations of the four parameters, $\alpha(=|J'|/J)$, $\beta(=S'/S)$, $\delta(=D/Jz)$ and $\delta'(=D'/Jz)$. Here J and D are respectively the exchange and anisotropy constants of the host and S is a magnitude of its spin. J', D' and S' are associated with the impurity, and z is the number of nearest neighbors. It is shown that we can expect localized modes in the anisotropy energy gap as well as above and below the spin-wave energy continuum for suitable values of the parameters. The results are applied to discuss an Mn^{2+} impurity in the antiferromagnetic FeF_2. The zero point contraction of the impurity and its nearest neighboring spins is calculated in the antiferromagnetic impurity case. It is found that, as a function of α and β, the nearest neighboring spin contraction has an oscillatory behavior.

§ 1. Introduction

The magnetic impurity problem is one of a class of problems concerning the effects of impurities on the continuous energy spectra of elementary excitations in solids. Here we are concerned with the effect of an impurity on the magnon spectrum. The impurity problem for spin-wave excitations in magnetic materials has been studied extensively in recent years. In 1963 Wolfram and Callaway,[1] Takeno,[2] and Li and Zhu[3] examined independently the effect of a single substituted impurity spin on the spin-wave spectrum of a Heisenberg ferromagnet with nearest neighbor interactions only. They treated the case in which an impurity spin has a spin different from the host spins and interacts ferromagnetically with its nearest neighbors by an exchange integral different from that between nearest neighboring pairs of host spins. The corresponding problem for an antiferromagnetically coupled impurity spin in an otherwise ferromagnetic material was developed later by Ishii, Kanamori and Nakamura.[4] For a physical interpretation of the above theories the reader is referred to reference 5).

*) Present address: Department of Physics, Faculty of Science, Kobe University, Rokkodai, Kobe.

The main purpose of the present paper is to discuss theoretically the localized spin-wave modes in a Heisenberg antiferromagnet with a single substituted impurity spin. The case which we consider is a simple Heisenberg spin Hamiltonian with an intersublattice exchange interaction only, plus an anisotropy term of the form $-DS_z^2$. Both the cases of a ferromagnetically and antiferromagnetically coupled impurity spin will be studied. The spin as well as the exchange and anisotropy constants of the impurity may differ from those of the host. The spin-wave approximation is introduced by reducing the Hamiltonian to quadratic terms in the Holstein-Primakoff[6] Boson creation and annihilation operators. The method of diagonalizing this Hamiltonian is similar to that used by Ishii et al.[4] In numerical calculations we confine ourselves to the body-centered cubic and MnF_2 (rutile)-type lattices, which are topologically equivalent to each other in the present case.

In reference 5) the present author and Kanamori dealt with the general aspects of the present problem and gave a part of the numerical results for the special case where anisotropy is absent. Here we discuss the problem in more detail and include the $-DS_z^2$ term. When anisotropy is present, there is a gap in the spin-wave frequency continuum around zero frequency. We consider the modes which appear in this gap as well as the more familiar modes analogous to those which occur in the $D=0$ case. Numerical results of the localized spin-wave problem are applied to discuss an Mn^{2+} impurity in the antiferromagnetic crystal FeF_2. We also discuss the zero point contraction of the impurity spin and its neighbors. Recently the same problem was also studied independently by Lovesey.[7] Some of the results in the present paper overlap those obtained by him.

In § 2, we develop the formulation for the spin-wave impurity problem in an antiferromagnet with a single substituted impurity spin. In § 3, numerical calculations both of the criteria for the appearance of the various types of localized modes and of their energies are presented in detail. Applications of the results to a real substance are then given in § 4. Section 5 is concerned with the theoretical study of the zero point contraction of the impurity and its nearest neighboring spins. The last section (§ 6) is devoted to concluding remarks. In the Appendix, we discuss the analytical forms of the Green's functions and give some relations among them which are used in the text. We further discuss the method of numerical calculation of the Green's functions and present tables of the results.

§ 2. Formulation of the spin-wave impurity problem in an antiferromagnet

We treat a simple two-sublattice antiferromagnet with a single substituted impurity spin. The basic Hamiltonian is given by

$$\mathcal{H}=2J\sum_{j(\neq 0)}\sum_{\rho}\boldsymbol{S}_j\cdot\boldsymbol{S}_{j+\rho}+2J'\sum_{\rho}\boldsymbol{S}_0\cdot\boldsymbol{S}_{\rho} \\ -D\sum_{j(\neq 0)}(S_j^z)^2-D\sum_{l}(S_l^z)^2-D'(S_0^z)^2, \tag{2·1}$$

where $\boldsymbol{S}_j$ and $\boldsymbol{S}_l$ denote the atomic spins associated with the j-th and l-th atoms, respectively. The sum over j runs over sites of the up sublattice, and it is assumed that the nearest neighbors of j, $j+\rho$, are on the opposite sublattice and thus point in the negative z direction. The sum over l runs over sites of the down sublattice. We further assume that the impurity spin is at the origin of coordinates ($j=0$) and thus belongs to the sublattice formed by the positive spins. The first term in Eq. (2·1) represents the antiferromagnetic exchange interaction between nearest neighboring host spins ($J>0$), and the second term represents that between the impurity spin and its nearest neighbors. We treat both the $J'>0$ case (antiferromagnetic impurity) and the $J'<0$ case (ferromagnetic impurity). When J' is positive the impurity spin is parallel to the positive z direction, and when J' is negative it is parallel to the negative z direction. The last three terms represent the uniaxial anisotropy energies of the host and impurity spins. The signs of D and D' are taken as positive.*)

(*A*) *The antiferromagnetic impurity case* ($J'>0$)

Following the Holstein-Primakoff formalism[6] for a two-sublattice antiferromagnet, we introduce the Boson creation and annihilation operators, a_j^*, b_l^*, a_j and b_l, and expand the Hamiltonian keeping terms up to second order:**)

$$\mathcal{H}=2JSz\{\sum_{j(\neq 0)}a_j^*a_j+\sum_{l(\neq\rho)}b_l^*b_l\}+2JS(z-1)\sum_{\rho}b_{\rho}^*b_{\rho} \\ +2J'Sza_0^*a_0+2J'S'\sum_{\rho}b_{\rho}^*b_{\rho} \\ +2JS\sum_{\substack{j,\rho\\(j\neq 0)}}(a_jb_{j+\rho}+a_j^*b_{j+\rho}^*) \\ +2J'(SS')^{1/2}\sum_{\rho}(a_0b_{\rho}+a_0^*b_{\rho}^*) \\ +2DS\{\sum_{j(\neq 0)}a_j^*a_j+\sum_{l}b_l^*b_l\}+2D'S'a_0^*a_0\,. \tag{2·2}$$

Here S and S' are respectively the magnitudes of the host and impurity spins, and z stands for the number of nearest neighbors. The commutation relations among the Boson operators are

*) The treatment which follows is also applicable for $D'<0$, as long as the z axis remains a stable direction for the impurity spin.

**) In the Hamiltonian of Eq. (2·2) the anisotropy energy terms do not vanish for the spin whose magnitude is one half. This situation comes from the fact that we take here the linear spin-wave approximation. This contradiction can be avoided by regarding D and D' in Eq. (2·2) (and thus those which will appear hereafter) as $(2S-1)/2S$ times D in Eq. (2·1) and $(2S'-1)/2S'$ times D' in Eq. (2·1) respectively.

$$[a_j, a_{j'}^*] = \delta_{j,j'}, \qquad [b_l, b_{l'}^*] = \delta_{l,l'}, \tag{2·3}$$

and all other commutation relations are zero. By use of a method similar to that of Ishii et al.,[4] this quadratic Hamiltonian can be diagonalized straightforwardly. We consider a new operator c_λ which is given by

$$c_\lambda = \sum_j \Gamma_j^\lambda a_j + \sum_l \Gamma_l^\lambda b_l^*. \tag{2·4}$$

A set of secular equations which determine the eigenvalues E_λ and the coefficients Γ_j^λ and Γ_l^λ is obtained by the following equation:

$$[\mathcal{H}, c_\lambda] = -E_\lambda c_\lambda. \tag{2·5}$$

With the use of Eqs. (2·2), (2·3), (2·4) and (2·5) the secular equations become as follows:

$$\{-E_\lambda + 2S(Jz+D)\}\Gamma_0^\lambda - 2JS\sum_{\rho'}\Gamma_{\rho'}^\lambda = -2Sz(J'-J)\Gamma_0^\lambda - 2(D'S'-DS)\Gamma_0^\lambda + 2(J'\sqrt{SS'}-JS)\sum_{\rho'}\Gamma_{\rho'}^\lambda, \tag{2·6a}$$

$$\{-E_\lambda + 2S(Jz+D)\}\Gamma_j^\lambda - 2JS\sum_{\rho'}\Gamma_{j+\rho'}^\lambda = 0, \qquad (j\neq 0) \tag{2·6b}$$

$$\{-E_\lambda - 2S(Jz+D)\}\Gamma_\rho^\lambda + 2JS\sum_{\rho'}\Gamma_{\rho-\rho'}^\lambda = 2(J'S'-JS)\Gamma_\rho^\lambda - 2(J'\sqrt{SS'}-JS)\Gamma_0^\lambda, \tag{2·6c}$$

$$\{-E_\lambda - 2S(Jz+D)\}\Gamma_l^\lambda + 2JS\sum_{\rho'}\Gamma_{l-\rho'}^\lambda = 0. \qquad (l\neq\rho) \tag{2·6d}$$

Note that Eqs. (2·6a) and (2·6c) show the perturbation of the periodic nature of the system. If the eigenvalue, E_λ, obtained from these secular equations is positive, then we may identify the operator c_λ with the annihilation operator associated with the resulting mode such that

$$c_\lambda|0\rangle = 0, \tag{2·7}$$

where $|0\rangle$ is the ground state wave function of the system. If the eigenvalue E_λ is negative, on the other hand, the annihilation operator may be defined by c_λ^* which is the Hermitian conjugate of the right-hand side of Eq. (2·4). In both cases the excitation energy is positive, and it is the absolute value of E_λ.

Now, we introduce the crystal Green's functions defined as follows:

$$G(j, j'; E) = \frac{1}{N}\sum_{\boldsymbol{k}}\frac{p_{\boldsymbol{k}+}p_{\boldsymbol{k}+}e^{i\boldsymbol{k}\cdot(\boldsymbol{R}_j-\boldsymbol{R}_{j'})}}{E_{\boldsymbol{k}+}^{(0)}-E} - \frac{1}{N}\sum_{\boldsymbol{k}}\frac{p_{\boldsymbol{k}-}p_{\boldsymbol{k}-}e^{i\boldsymbol{k}\cdot(\boldsymbol{R}_j-\boldsymbol{R}_{j'})}}{E_{\boldsymbol{k}-}^{(0)}-E}, \tag{2·8a}$$

$$G(j, l'; E) = \frac{1}{N}\sum_{\boldsymbol{k}}\frac{p_{\boldsymbol{k}-}q_{\boldsymbol{k}-}e^{i\boldsymbol{k}\cdot(\boldsymbol{R}_j-\boldsymbol{R}_{l'})}}{E_{\boldsymbol{k}-}^{(0)}-E} - \frac{1}{N}\sum_{\boldsymbol{k}}\frac{p_{\boldsymbol{k}+}q_{\boldsymbol{k}+}e^{i\boldsymbol{k}\cdot(\boldsymbol{R}_j-\boldsymbol{R}_{l'})}}{E_{\boldsymbol{k}+}^{(0)}-E}, \tag{2·8b}$$

$$G(l, j'; E) = \frac{1}{N}\sum_{\boldsymbol{k}}\frac{q_{\boldsymbol{k}+}p_{\boldsymbol{k}+}e^{i\boldsymbol{k}\cdot(\boldsymbol{R}_l-\boldsymbol{R}_{j'})}}{E_{\boldsymbol{k}+}^{(0)}-E} - \frac{1}{N}\sum_{\boldsymbol{k}}\frac{q_{\boldsymbol{k}-}p_{\boldsymbol{k}-}e^{i\boldsymbol{k}\cdot(\boldsymbol{R}_l-\boldsymbol{R}_{j'})}}{E_{\boldsymbol{k}-}^{(0)}-E}, \tag{2·8c}$$

$$G(l, l'; E) = \frac{1}{N}\sum_{\boldsymbol{k}} \frac{q_{\boldsymbol{k}-} q_{\boldsymbol{k}-} e^{i\boldsymbol{k}\cdot(\boldsymbol{R}_l - \boldsymbol{R}_{l'})}}{E^{(0)}_{\boldsymbol{k}-} - E} - \frac{1}{N}\sum_{\boldsymbol{k}} \frac{q_{\boldsymbol{k}+} q_{\boldsymbol{k}+} e^{i\boldsymbol{k}\cdot(\boldsymbol{R}_l - \boldsymbol{R}_{l'})}}{E^{(0)}_{\boldsymbol{k}+} - E}. \tag{2·8d}$$

Here N is the number of spins in the sublattice, $\boldsymbol{R}_j$ and $\boldsymbol{R}_l$ the lattice vectors connecting the origin with the j-th and l-th sites respectively, and $\boldsymbol{k}$ the wave vector. The summation with respect to $\boldsymbol{k}$ is taken over the first Brillouin zone. $E^{(0)}_{\boldsymbol{k}\pm}$, $p_{\boldsymbol{k}\pm}$ and $q_{\boldsymbol{k}\pm}$ are defined by

$$E^{(0)}_{\boldsymbol{k}\pm} = \pm 2S\sqrt{(Jz+D)^2 - J^2\gamma_{\boldsymbol{k}}{}^2}, \tag{2·9}$$

$$p_{\boldsymbol{k}\pm} = \left\{\frac{2S(Jz+D) + E^{(0)}_{\boldsymbol{k}\pm}}{\pm 2E^{(0)}_{\boldsymbol{k}\pm}}\right\}^{1/2}, \tag{2·10a}$$

$$q_{\boldsymbol{k}\pm} = \left\{\frac{2S(Jz+D) - E^{(0)}_{\boldsymbol{k}\pm}}{\pm 2E^{(0)}_{\boldsymbol{k}\pm}}\right\}^{1/2}, \tag{2·10b}$$

where

$$\gamma_{\boldsymbol{k}} = \sum_{\rho} e^{i\boldsymbol{k}\cdot\boldsymbol{R}_\rho}. \tag{2·11}$$

Note that $E^{(0)}_{\boldsymbol{k}\pm}$ is just the spin-wave spectrum in a pure antiferromagnet. The solutions of the set of secular equations (2·6a, b, c, d) may be written as follows:*)

$$\Gamma_j = V_0 G(j, 0; E) + \sum_{\rho} V_\rho G(j, \rho; E), \tag{2·12a}$$

$$\Gamma_l = V_0 G(l, 0; E) + \sum_{\rho} V_\rho G(l, \rho; E). \tag{2·12b}$$

Equations (2·6b) and (2·6d) are automatically satisfied by these Γ_j and Γ_l. Furthermore, by substituting Eqs. (2·12a, b) into Eqs. (2·6a, c), we can get the following new $z+1$ secular equations:

$$\begin{aligned} &V_0[1 + \{2(J'-J)Sz + 2(D'S'-DS)\}G(0, 0; E) \\ &\qquad - 2(J'\sqrt{SS'} - JS)zG(\rho, 0; E)] \\ &\quad + \sum_{\rho'} V_{\rho'}[\{2(J'-J)Sz + 2(D'S'-DS)\}G(0, \rho; E) \\ &\qquad - 2(J'\sqrt{SS'} - JS)\sum_{\rho''} G(\rho, \rho''; E)] = 0, \end{aligned} \tag{2·13a}$$

$$\begin{aligned} &V_0[-2(J'S'-JS)G(\rho, 0; E) + 2(J'\sqrt{SS'} - JS)G(0, 0; E)] \\ &\quad + \sum_{\rho'} V_{\rho'}[\delta_{\rho\rho'} - 2(J'S'-JS)G(\rho, \rho'; E) \\ &\qquad + 2(J'\sqrt{SS'} - JS)G(0, \rho; E)] = 0, \end{aligned} \tag{2·13b}$$

which determine V_0, V_ρ and the eigenvalues E. In deriving Eqs. (2·13a, b) we have used the fact that, in cubic lattices, $G(\rho, 0; E)$, $G(0, \rho; E)$ and $\sum_{\rho'} G(\rho, \rho'; E)$ are independent of the direction of the nearest neighboring vector, $\boldsymbol{R}_\rho$. Equations (2·13a, b) are the basic secular equations which determine the nature of

*) Hereafter the subscript λ will be omitted.

the spin-wave impurity state in an antiferromagnet with an antiferromagnetically coupled impurity spin.

Now, we will find solutions of Eqs. (2·13a, b). If we combine Eq. (2·13a) with the equation obtained by summing Eq. (2·13b) over ρ, the following equation, which determines the energy of the solution for non-zero V_0 and $\sum_\rho V_\rho$, can be obtained:

$$\begin{aligned} D_s^{AF}(\varepsilon) = \Gamma(0,0;\delta;\varepsilon)\Big[&\frac{1}{1+\delta}(\alpha-1+\beta\delta'-\delta) \\ &+\{\alpha\beta+\alpha-2-(\alpha\beta-1)(\beta\delta'-\delta)\}(\varepsilon-1) \\ &+(\alpha\beta-1)(1+\delta)(\varepsilon-1)^2\Big] \qquad (2\cdot14) \\ +\alpha\beta+\alpha-1&-(\alpha\beta-1)(\beta\delta'-\delta) \\ &+(\alpha\beta-1)(1+\delta)(\varepsilon-1) \\ =0\,,& \end{aligned}$$

where

$$\alpha=|J'|/J\,,\quad \beta=S'/S\,,\quad \delta=D/Jz\,,\quad \delta'=D'/Jz\,, \qquad (2\cdot15)$$

$$\varepsilon=E/2S(Jz+D)\,, \qquad (2\cdot16)$$

$$\Gamma(m,m';\delta;\varepsilon)=2S(Jz+D)G(m,m';E)\,, \qquad (2\cdot17)$$

$$(m=j,l;\ m'=j',l')$$

and where we have used the relations among the Green's functions which are given in the Appendix [see Eqs. (A·3a, b)]. We can easily show that, for this solution, the V_ρ's are independent of ρ in cases of cubic lattices. In other words, the solution with non-zero V_0 and $\sum_\rho V_\rho$ is of s type character. As is shown in the Appendix, the dimensionless Green's functions, Γ's, are functions of δ as well as ε. This is explicitly indicated in Eq. (2·17).

The other solutions can be obtained by putting $V_0=\sum_\rho V_\rho=0$ in Eq. (2·13b). The set of secular equations for these solutions thus becomes

$$\sum_{\rho'} V_{\rho'}[\delta_{\rho\rho'}-2(J'S'-JS)G(\rho,\rho';E)]=0\,. \qquad (2\cdot18)$$

The discussion which has been developed thus far in this section can be applied to all cases of cubic lattices. Hereafter we shall confine ourselves to the body-centered cubic lattice. In this lattice there exist eight nearest neighboring vectors which are specified by $\boldsymbol{R}_\rho=(n_xa/2,\ n_ya/2,\ n_za/2)$, where $|n_x|$, $|n_y|$ and $|n_z|$ are equal to unity and a is the lattice constant. If we use the symmetry property that $G(\rho,\rho';E)$ depends only on $|\boldsymbol{R}_\rho-\boldsymbol{R}_{\rho'}|$, then seven types of solutions can be derived from Eq. (2·18). Three of these solutions are of the p_x, p_y and p_z types. These three p type modes are degenerate, with energy determined from

$$D_p(\varepsilon)=1-\frac{\alpha\beta-1}{(1+\delta)z}\{\Gamma(111,\,111;\,\delta;\,\varepsilon)+\Gamma(111,\,11-1;\,\delta;\,\varepsilon)$$
$$-\Gamma(111,\,1-1-1;\,\delta;\,\varepsilon)-\Gamma(111,\,-1-1-1;\,\delta;\,\varepsilon)\}$$
$$=0\,. \tag{2·19}$$

Three other solutions are of the d_{yz}, d_{zx} and d_{xy} types. These d type modes are also degenerate. The energy is determined from

$$D_d(\varepsilon)=1-\frac{\alpha\beta-1}{(1+\delta)z}\{\Gamma(111,\,111;\,\delta;\,\varepsilon)-\Gamma(111,\,11-1;\,\delta;\,\varepsilon)$$
$$-\Gamma(111,\,1-1-1;\,\delta;\,\varepsilon)+\Gamma(111,\,-1-1-1;\,\delta;\,\varepsilon)\}$$
$$=0\,. \tag{2·20}$$

Lastly, there is an f_{xyz} type solution. The energy of this f type mode is a root of the equation

$$D_f(\varepsilon)=1-\frac{\alpha\beta-1}{(1+\delta)z}\{\Gamma(111,\,111;\,\delta;\,\varepsilon)-3\Gamma(111,\,11-1;\,\delta;\,\varepsilon)$$
$$+3\Gamma(111,\,1-1-1;\,\delta;\,\varepsilon)-\Gamma(111,\,-1-1-1;\,\delta;\,\varepsilon)\}$$
$$=0\,. \tag{2·21}$$

As seen from Eqs. (2·19), (2·20) and (2·21), the energies of the p, d and f modes are independent of the value of D'. This is because the impurity spin does not participate in the precessional motion. Numerical analysis of Eqs. (2·14) (for the body-centered cubic lattice), (2·19), (2·20) and (2·21) will be given in the next section.

(*B*) *The ferromagnetic impurity case* ($J'<0$)

In the present case an impurity spin points in the negative z direction. The quadratic Hamiltonian thus becomes

$$\begin{aligned}\mathcal{H}=&2JSz\{\sum_{j(\neq 0)}a_j^*a_j+\sum_{l(\neq\rho)}b_l^*b_l\}+2JS(z-1)\sum_{\rho}b_\rho^*b_\rho\\&+2|J'|Sza_0^*a_0+2|J'|S'\sum_{\rho}b_\rho^*b_\rho\\&+2JS\sum_{\substack{j,\rho\\(j\neq 0)}}(a_jb_{j+\rho}+a_j^*b_{j+\rho}^*)\\&-2|J'|(SS')^{1/2}\sum_{\rho}(a_0b_\rho^*+a_0^*b_\rho)\\&+2DS\{\sum_{j(\neq 0)}a_j^*a_j+\sum_{l}b_l^*b_l\}+2D'S'a_0^*a_0\,.\end{aligned} \tag{2·22}$$

Introducing a linear combination of Boson operators defined by

$$c_\lambda=\Gamma_0^\lambda a_0^*+\sum_{j(\neq 0)}\Gamma_j^\lambda a_j+\sum_{l}\Gamma_l^\lambda b_l^* \tag{2·23}$$

and using a method similar to that in the antiferromagnetic impurity case, we can diagonalize the above Hamiltonian (2·22). The resulting equation which determines the energy of the s type mode in this case is given by

$$\begin{aligned} D_s^F(\varepsilon) = \Gamma(0,0;\delta;\varepsilon) \Big[& -\frac{1}{1+\delta}(\alpha+1+\beta\delta'+\delta) \\ & + \{\alpha\beta-\alpha-2+(\alpha\beta-1)(\beta\delta'+\delta)\}(\varepsilon-1) \\ & + (\alpha\beta-1)(1+\delta)(\varepsilon-1)^2 \Big] \\ + \alpha\beta-\alpha-1 & + (\alpha\beta-1)(\beta\delta'+\delta) \\ & + (\alpha\beta-1)(1+\delta)(\varepsilon-1) \\ = 0 & . \end{aligned} \tag{2·24}$$

This equation is valid for all cases of cubic lattices. In the next section we will solve Eq. (2·24) numerically for the body-centered cubic lattice. The equations for other (p, d and f) modes are the same as those in the antiferromagnetic impurity case.

§ 3. Numerical calculations and discussion

In this section we give the numerical analysis of Eqs. (2·14), (2·19), (2·20), (2·21) and (2·24) which determine the energies of the various types of localized modes. We can easily show that all of $D(\varepsilon)$'s approach unity as ε tends to $\pm\infty$. This fact will be used later when we discuss the criteria for the existence of the localized spin-wave modes.

(A) *The case* $\delta=\delta'=0$

Now, let us discuss the case where δ and δ' are equal to zero. In this case the spin-wave energy band extends from $\varepsilon=1$ to $\varepsilon=-1$ [see Eqs. (2·9) and (2·16)]. First we look for the solutions of Eq. (2·14). Careful examination of the ε-dependence of $D_s^{AF}(\varepsilon)$ shows that Eq. (2·14) has one solution at most in the region $\varepsilon>1$ and also in the region $\varepsilon<-1$. Thus the criterion for the appearance of the localized s_0 mode*) with the energy $\varepsilon>1$ (above the spin-wave energy continuum) is $D_s^{AF}(1)<0$, or more conveniently,

$$\alpha-1>0 . \tag{3·1}$$

(Remember here that $D_s^{AF}(\varepsilon)$ goes to unity as $\varepsilon\to+\infty$.) Here we have used the fact that the Green's function $\Gamma(0,0;\delta;\varepsilon)$ has the asymptotic form $-[(1+\delta)/2\pi^2]\cdot\sqrt{(\varepsilon+1)/(\varepsilon-1)}\cdot[\log(\varepsilon^2-1)]^2$ at $|\varepsilon|=1_{+0}$. Note that the condition (3·1) is independent of β. Similarly the localized s_1 mode*) appears below the continuum

*) Hereafter the s modes with positive and negative energies in the antiferromagnetic impurity case are called the s_0 and s_1 modes, respectively. As regards the physical distinction between these two modes see reference 5).

on the negative energy side ($\varepsilon<-1$) when $D_s^{AF}(-1)<0$. This is equivalent to

$$1+\alpha-\alpha\beta<0\,. \tag{3·2}$$

Next we discuss Eq. (2·24). Calculation shows that Eq. (2·24) has no solutions in the region $\varepsilon>1$. On the other hand, it has one solution at most in the region $\varepsilon<-1$. Thus the s type mode in the ferromagnetic impurity case can be localized only below the spin-wave energy continuum under the condition $D_s^{F}(-1)<0$, or

$$1-\alpha-\alpha\beta<0\,. \tag{3·3}$$

This s type mode is in some sense an amalgam of the s_0 and s_1 modes in the antiferromagnetic impurity case.*)

Finally we consider Eqs. (2·19, 20, 21). From these equations we can show that for each of the p, d and f modes one localized mode at most also appears only below the spin-wave energy continuum on the negative energy side. The criteria for the appearance of these localized modes are $D_p(-1)<0$, $D_d(-1)<0$ and $D_f(-1)<0$ for the p, d and f modes respectively. Since all of the linear combinations of $\Gamma(\rho, \rho'; \delta; \varepsilon)$ which appear in the brackets of Eqs. (2·19, 20, 21) diverge as ε approaches -1 from the negative infinite side, these three conditions coincide and are given by

$$\alpha\beta-1>0\,. \tag{3·4}$$

The boundary curves in the α-β plane for the appearance of the various types of localized modes, which were discussed above, may be found in Fig. 1 in reference 5). It is worth mentioning that for $\beta\leqq 1$ we have no localized s_1 mode in the antiferromagnetic impurity case. All other localized modes, on the other hand, may appear for any value of β. In Figs. 1 and 2 we give the iso-energy curves of the localized s_0 and s_1 modes, which are obtained from Eq. (2·14) (the antiferromagnetic impurity case). We also give the iso-energy curves of the s type localized mode in the ferromagnetic impurity case in Fig. 3, and those of the p, d and f type localized modes in Fig. 4. These iso-energy curves are obtained from Eqs. (2·24, 19, 20, 21), respectively. In the numerical calculations we have used the values listed in Table I in the Appendix. The method by which these values are calculated is discussed in detail in the Appendix.

As seen in Fig. 1, the energy of the localized s_0 mode at $\beta=0$ is α ($=2J'Sz/2JSz$), which is the value expected in the molecular field approximation. (As was discussed in reference 5), in the s_0 mode most of the spin-wave amplitude is associated with the impurity spin.) This result is quite natural, since the coefficient of the $a_0 b_\rho$ and $a_0{}^* b_\rho{}^*$ terms in the Hamiltonian of Eq. (2·2) is $\alpha\sqrt{\beta}/z$ in the unit of $2JSz$ and thus these terms vanish when $\beta=0$. Therefore,

*) See reference 5).

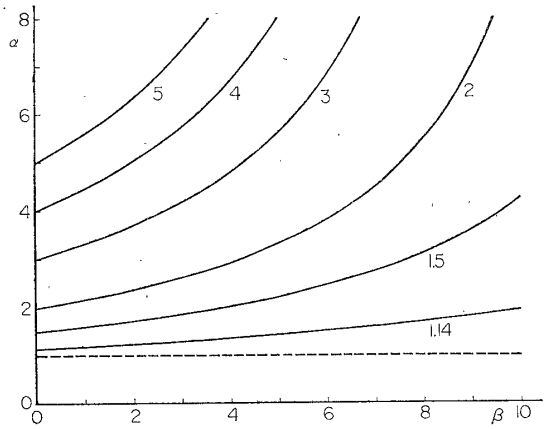

Fig. 1. Iso-energy curves of the localized s_0 mode which occurs above the band ($\varepsilon>1$) in the antiferromagnetic impurity case for $\delta=\delta'=0$. The numerical figures denote the energy, ε, of the localized s_0 mode. The boundary curve for the appearance of this localized mode is also given; it is shown by the dotted curve.

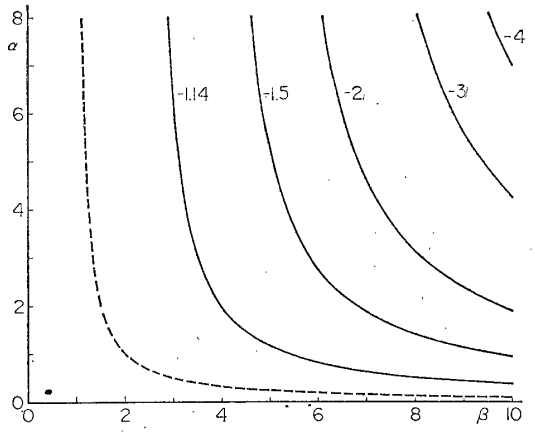

Fig. 2. Same as Fig. 1 for the localized s_1 mode below the band ($\varepsilon<-1$) in the antiferromagnetic impurity case.

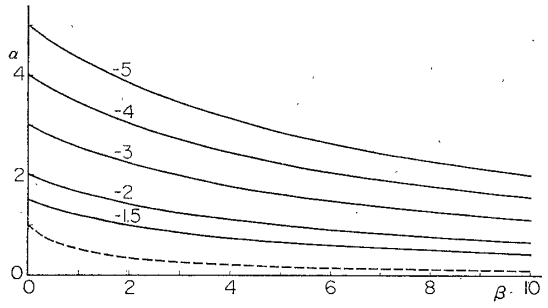

Fig. 3. Same as Fig. 1 for the localized s mode below the band ($\varepsilon<-1$) in the ferromagnetic impurity case.

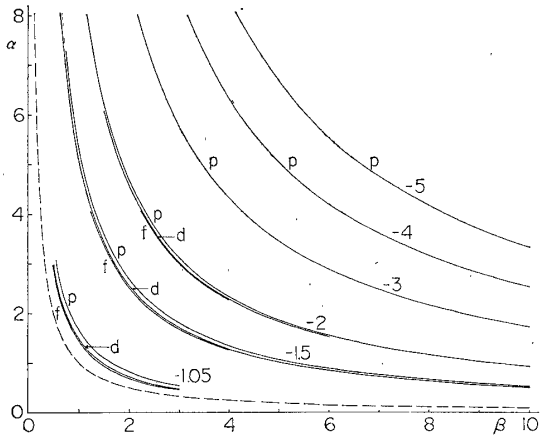

Fig. 4. Same as Fig. 1 for the localized p, d and f modes below the band ($\varepsilon<-1$).

when $\beta=0$, the impurity spin precesses independently of its neighboring spins under the effective magnetic field, $2J'Sz/2JSz$. For $\beta\neq0$ the result differs from the molecular field approximation, and thus the energy of the localized s_0 mode depends on β. This dependence is, however, rather weak provided α and β are not too large. This point has also been discussed by Lovesey.[7] The excitation energy of the localized s mode in the ferromagnetic impurity case is also α when $\beta=0$ (see Fig. 3). This shows that the nature of this localized mode for sufficiently small values of β resembles that of the localized s_0 mode in the antiferromagnetic impurity case. Finally we note that for fixed α and β the excitation energies of the localized p, d and f modes are relatively close with the p mode always lowest, followed by the d and f modes in that order.

(*B*) *The case* $\delta>0$ *and* $\delta'\geqq0$

In this case there exists a gap in the spin-wave energy continuum, the range

of which can be calculated from Eqs. (2·9) and (2·16) to be $|\varepsilon|<\varepsilon_b=\sqrt{2\delta+\delta^2}/(1+\delta)$. For now we confine ourselves to the localized modes which appear in this gap. First we discuss the s type localized modes in the antiferromagnetic impurity case. From Eq. (2·14) we can easily show that $D_s^{AF}(0)\geqq 0$. (Equality is achieved only when $\alpha=\beta\delta'=0$.) Thus, by examining the ε-dependence of $D_s^{AF}(\varepsilon)$, we can conclude that one localized s_0 mode with energy, $0<\varepsilon<\varepsilon_b$, appears in the gap under the condition that*)

$$\begin{aligned} D_s^{AF}(+\varepsilon_b) = &-\alpha\beta\cdot(W-1)\cdot\{\sqrt{2\delta+\delta^2}-\beta\delta'\} \\ &+\alpha\{\delta\cdot W+\sqrt{2\delta+\delta^2}\cdot W+1\} \\ &-\{\delta\cdot W+\sqrt{2\delta+\delta^2}\cdot W+1\}\cdot\{\sqrt{2\delta+\delta^2}-\beta\delta'\} \\ <&0\,, \end{aligned} \tag{3·5}$$

where W is defined by

$$\Gamma(0,\,0;\,\delta;\,+\varepsilon_b)=(1+\delta+\sqrt{2\delta+\delta^2})\cdot(1+\delta)\cdot W\,. \tag{3·6}$$

Thus, W is the value of $\Gamma(0,\,0;\,0;\,0)$ and was calculated by Watson[8] as 1.3932. Similarly we can get the following equation for the criterion for the appearance of the localized s_1 mode in the region $-\varepsilon_b<\varepsilon<0$:

$$\begin{aligned} D_s^{AF}(-\varepsilon_b) = &\alpha\beta\cdot(W-1)\cdot\{\sqrt{2\delta+\delta^2}+\beta\delta'\} \\ &+\alpha\{\delta\cdot W-\sqrt{2\delta+\delta^2}\cdot W+1\} \\ &+\{\delta\cdot W-\sqrt{2\delta+\delta^2}\cdot W+1\}\cdot\{\sqrt{2\delta+\delta^2}+\beta\delta'\} \\ <&0\,. \end{aligned} \tag{3·7}$$

The condition (3·5) is achieved only when $\sqrt{2\delta+\delta^2}-\beta\delta'>0$. Thus, if $\sqrt{2\delta+\delta^2}\leqq\beta\delta'$, there are no localized s_0 modes in the gap. The boundary curves of the regions in the α-β plane where the localized s_0 mode appears in the gap are shown by solid curves in Fig. 5 for representative values of δ and $\beta\delta'$.**) This mode appears in the gap for parameters in the region below each boundary curve. In Fig. 6 we show the iso-energy curves of the mode obtained from Eq. (2·14) and the values listed in Table I for $\delta=0.3$ and $\beta\delta'=0.0$ and 0.1.**) We see that when β goes to zero the energy of the localized s_0 mode approaches $(\alpha+\beta\delta')/(1+\delta)$ $[=2(J'Sz+D'S')/2S(Jz+D)]$, as would be expected from the argument mentioned earlier about the energy of the s_0 mode in the case $\delta=\delta'=0$. We also see that the energy of this mode in the gap depends weakly on β if β is small. Furthermore, when the values of δ and $\beta\delta'$ are fixed, the minimum value of the energy is $\beta\delta'/(1+\delta)$. In other words, even when the impurity-host exchange interaction vanishes (i.e. $\alpha=0$), the energy of the localized s_0 mode

*) The case $\alpha=\beta\delta'=0$ is included in this condition.

**) Boundary and iso-energy curves for values other than those presented here may be obtained from the author upon request.

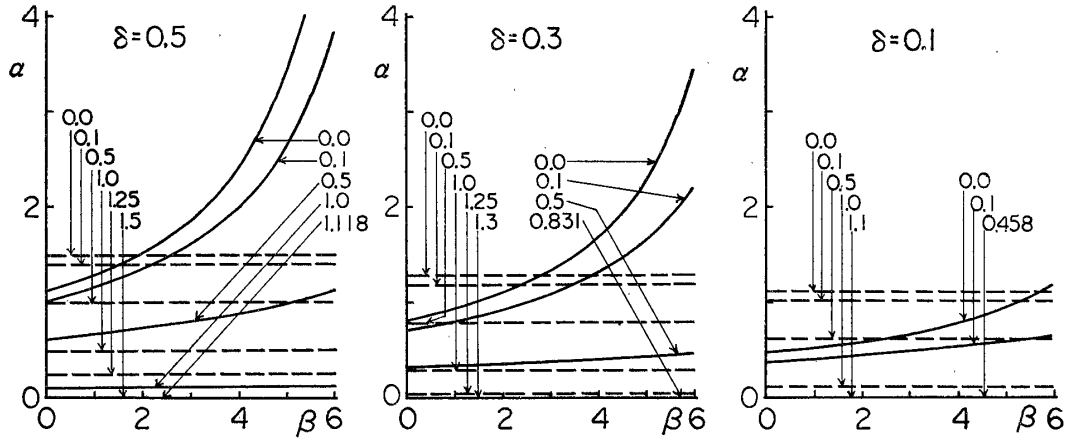

Fig. 5. Boundary curves for the appearance of localized s_0 modes above the spin-wave energy band ($\varepsilon>1$) and in the energy gap ($0<\varepsilon<\varepsilon_b$) in the antiferromagnetic impurity case for representative values of $\delta(>0)$ and $\beta\delta'(\geqq 0)$. Numerical figures denote the values of $\beta\delta'$. A localized s_0 mode appears above the band for α, β above the dotted boundary curves. A mode occurs in the gap for α, β below the solid boundary curves. Note that one localized s_0 mode always occurs above the band when $\beta\delta'>(1+\delta)$ and also that there is never an s_0 mode in the gap when $\beta\delta'\geqq\sqrt{2\delta+\delta^2}$. These critical values of $\beta\delta'$ are therefore just the values at which the abscissae become the corresponding boundary curves.

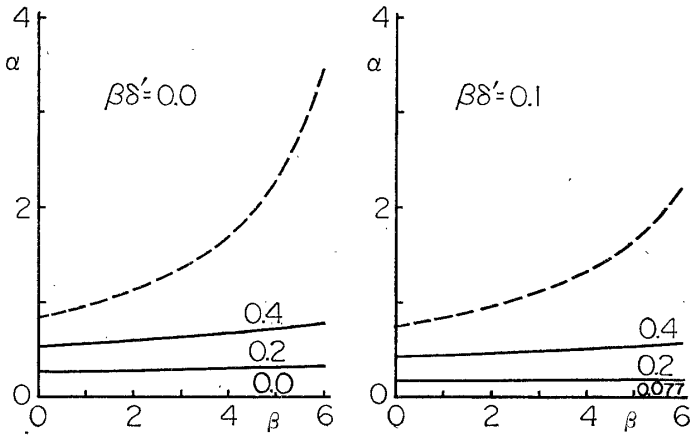

Fig. 6. Iso-energy curves of the localized s_0 mode in the energy gap ($0<\varepsilon<\varepsilon_b$) in the antiferromagnetic impurity case for $\delta=0.3$ and for $\beta\delta'=0.0$ and 0.1. The numerical figures denote the energy, ε, of the localized s_0 mode. The energy at $\alpha=0$ for fixed δ and $\beta\delta'$ is given by $\beta\delta'/(1+\delta)$. The boundary curves for the appearance of this localized mode are also shown by dotted curves.

is not zero but $\beta\delta'/(1+\delta)$. This is because when $\alpha=0$ the impurity spin precesses independently under an effective magnetic field which comes from the anisotropy energy at the impurity site. The energy, $\beta\delta'/(1+\delta)$, corresponds to this effective field. From this fact we can easily understand that the localized s_0 mode does not appear in the gap when $\beta\delta'\geqq\sqrt{2\delta+\delta^2}$, or equivalently, when $\beta\delta'/(1+\delta)\geqq\varepsilon_b$. On the other hand, the condition (3·7), for the appearance of

the localized s_1 mode, is achieved only when $\delta \cdot W - \sqrt{2\delta + \delta^2} \cdot W + 1 < 0$, or equivalently, $\delta > 1/2W(W-1) = 0.9127$. Furthermore, even when δ is larger than $1/2W(W-1)$, the energy of the localized s_1 mode is still only just above the spin-wave energy continuum.

Next we discuss the s type localized modes in the ferromagnetic impurity case. From Eq. (2·24) we can show that there exist no s type localized modes in the region of $0 < \varepsilon < \varepsilon_b$. For the s type localized modes with the energy, $-\varepsilon_b < \varepsilon \leqq 0$, on the other hand, the situation is somewhat complicated, since these modes are in some sense amalgams of the localized s_0 and s_1 modes of the antiferromagnetic impurity case. Now it is convenient to discuss Eq. (2·24) by examining the following four cases: (i) $\delta \leqq 1/2W(W-1)$ and $\beta\delta' \geqq \sqrt{2\delta + \delta^2}$, (ii) $\delta \leqq 1/2W(W-1)$ and $\beta\delta' < \sqrt{2\delta + \delta^2}$, (iii) $\delta > 1/2W(W-1)$ and $\beta\delta' \geqq \sqrt{2\delta + \delta^2}$ and (iv) $\delta > 1/2W(W-1)$ and $\beta\delta' < \sqrt{2\delta + \delta^2}$. In case (i) we have no s type localized modes in the gap.

In case (ii) one s type mode can be localized in the gap under the condition that

$$\begin{aligned} D_s^F(-\varepsilon_b) = {} & \alpha\beta \cdot (W-1) \cdot \{\sqrt{2\delta + \delta^2} - \beta\delta'\} \\ & - \alpha\{\delta \cdot W - \sqrt{2\delta + \delta^2} \cdot W + 1\} \\ & + \{\delta \cdot W - \sqrt{2\delta + \delta^2} \cdot W + 1\} \cdot \{\sqrt{2\delta + \delta^2} - \beta\delta'\} \\ > {} & 0 . \end{aligned} \tag{3·8}$$

For the given representative values of δ and $\beta\delta'$ this condition is satisfied in the region below the corresponding boundary curves which we indicate by solid curves in Fig. 7.*) In Fig. 8 we also indicate some iso-energy curves of the localized s mode in this case*). These curves are obtained from Eq. (2·24) and the values listed in Table I. The minimum excitation energy of the localized mode for fixed δ and $\beta\delta'$ is $|-\beta\delta'/(1+\delta)|$. As β goes to zero the localized mode energy approaches the function, $-(\alpha + \beta\delta')/(1+\delta)$. Thus it is clear that this localized s mode might have a nature similar to that of the localized s_0 mode in the antiferromagnetic impurity case. The only difference which we note here is that, when the values of δ and $\beta\delta'$ are fixed, the region of the appearance of the former mode is much wider than that of the latter mode (compare Fig. 7 with Fig. 5). This difference becomes more significant for larger δ and smaller $\beta\delta'$. When $\delta = 0.5$ and $\beta\delta' = 0$, the former mode appears in the gap for almost all region in the α-β plane except for a very narrow region near $\beta = 0$.

In case (iii) one s type localized mode, which resembles the localized s_1 mode in the antiferromagnetic impurity case, appears in the gap when $D_s^F(-\varepsilon_b) > 0$. Lastly, in case (iv), we have one s type localized mode in the gap when

*) See the second footnote on page 1205.

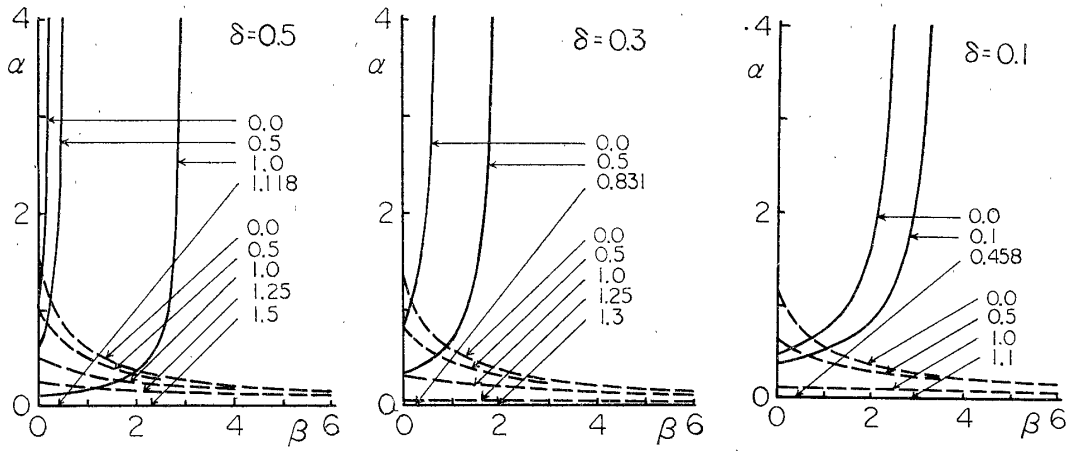

Fig. 7. Boundary curves for the appearance of localized s modes below the spin-wave energy band ($\varepsilon<-1$) and in the energy gap ($0>\varepsilon>-\varepsilon_b$) in the ferromagnetic impurity case for representative values of $\delta[0<\delta\leqq 1/2W(W-1)]$ and $\beta\delta'(\geqq 0)$ [see Eq. (3·6) for the definition of W]. Numerical figures denote the values of $\beta\delta'$. A localized s mode appears below the band for α, β above the dotted boundary curves. A mode occurs in the gap for α, β below the solid boundary curves. One localized s mode at least occurs below the band when $\beta\delta'>(1+\delta)$, and this kind of mode never occurs in the gap when $\beta\delta'\geqq\sqrt{2\delta+\delta^2}$ for δ smaller than or equal to $1/2W(W-1)$. These critical values of $\beta\delta'$ are therefore just the values at which the abscissae become the corresponding boundary curves.

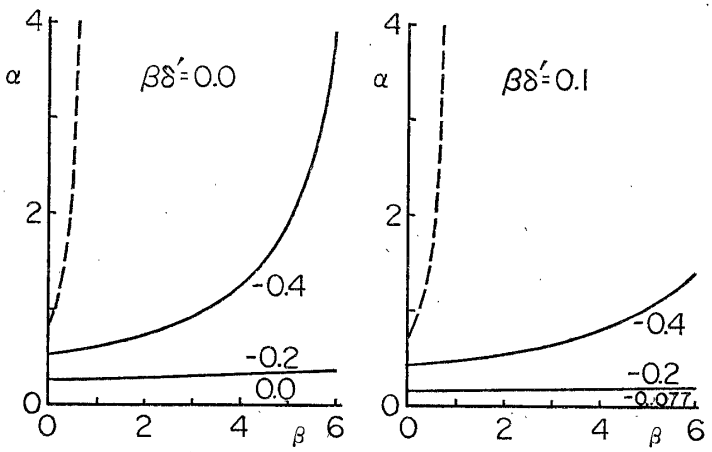

Fig. 8. Iso-energy curves of the localized s mode in the energy gap ($0>\varepsilon>-\varepsilon_b$) in the ferromagnetic impurity case for $\delta=0.3$ and for $\beta\delta'=0.0$ and 0.1. The numerical figures denote the energy, ε, of the localized s mode. The energy at $\alpha=0$ for fixed δ and $\beta\delta'$ is given by $-\beta\delta'/(1+\delta)$. The boundary curves for the appearance of this localized mode are also shown by dotted curves.

$D_s^F(-\varepsilon_b)\geqq 0$, and two s type localized modes in the gap when $D_s^F(-\varepsilon_b)<0$. These localized modes are amalgams of the localized s_0 and s_1 modes.

Finally we discuss the p, d and f type localized modes, the energies of which are determined from Eqs. (2·19), (2·20) and (2·21), respectively. Calculation shows that there exist no p, d and f type localized modes with the energy,

$0 \leqq \varepsilon < \varepsilon_b$. On the other hand, localized modes of these types can occur in the range, $0 > \varepsilon > -\varepsilon_b$, when δ is sufficiently large. The minimum values of δ are 2.2 for the p type mode, 2.8 for the d type and 3.0 for the f type.*) We cannot expect, however, such large values of δ in usual antiferromagnets. This completes the discussion of the localized spin-wave modes which occur in the energy gap.

Now we turn briefly to the discussion of the localized modes which appear above ($\varepsilon > 1$) and below ($\varepsilon < -1$) the spin-wave energy continuum. The criteria for the existence of localized modes in these regions are obtained by a method similar to that used previously in the discussion of the case $\delta = \delta' = 0$. In the antiferromagnetic impurity case, one localized s_0 mode occurs in the region, $\varepsilon > 1$, when

$$\alpha - 1 + \beta\delta' - \delta > 0 , \tag{3·9}$$

and one localized s_1 mode appears in the region, $\varepsilon < -1$, when

$$-\alpha\beta(1 + \delta + \beta\delta') + \alpha + 1 + \delta + \beta\delta' < 0 . \tag{3·10}$$

When $\delta = \delta' = 0$, Eq. (3·9) agrees with Eq. (3·1) and Eq. (3·10) agrees with Eq. (3·2). Note that one localized s_0 mode always occurs in the region, $\varepsilon > 1$, for values of δ and $\beta\delta'$ which satisfy the inequality, $\beta\delta'/(1+\delta)$ (minimum energy of the localized s_0 mode) > 1 (the energy at the top of the band). Note also that there exist no localized s_1 modes in the region, $\varepsilon < -1$, when β is less than or equal to $1/(1+\delta+\beta\delta')$. Several examples of boundary curves in the α-β plane for the appearance of the localized s_0 and s_1 modes, discussed above, are shown

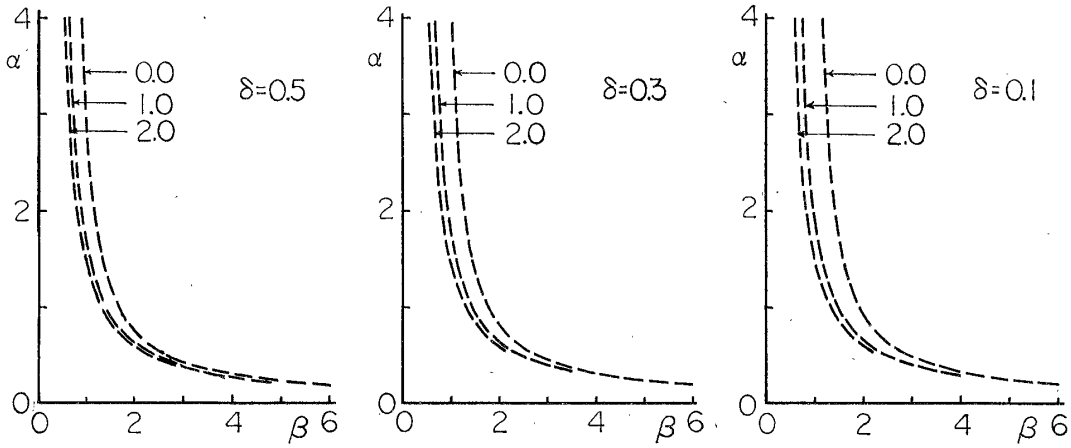

Fig. 9. Boundary curves for the appearance of the localized s_1 mode below the spin-wave energy band ($\varepsilon < -1$) in the antiferromagnetic impurity case for representative values of $\delta (> 0)$ and $\beta\delta' (\geqq 0)$. Numerical figures denote the values of $\beta\delta'$. One localized s_1 mode appears below the band for α, β above the dotted boundary curves.

*) These values are obtained by a method similar to that used to determine the minimum value of δ for the appearance of the localized s_1 mode with the energy, $-\varepsilon_b < \varepsilon < 0$. In the present case, however, the values of $\Gamma(111,111;\,0;\,0)$, $\Gamma(111,11-1;\,0;\,0)$, $\Gamma(111,1-1-1;\,0;\,0)$ and $\Gamma(111,-1-1-1;\,0;\,0)$ (see Table IIA in the Appendix) were employed.

by dotted curves in Fig. 5 and in Fig. 9, respectively.*) Each localized mode appears above its boundary curve. It should be noted here that, as can be seen from Fig. 5, there are regions in which two localized s_0 modes appear; one of which is in the gap and the other above the spin-wave energy band. Furthermore, from Fig. 9 we can see that, as expected, $\beta\delta'$ has much less effect on the boundary curves for the localized s_1 mode than on those for the localized s_0 mode.

Next we discuss the s type localized modes in the ferromagnetic impurity case. In the region, $\varepsilon>1$, we have no s type localized modes, as is in the case $\delta=\delta'=0$. In the region, $\varepsilon<-1$, on the other hand, one or two s type localized modes can occur. When $\beta\delta'/(1+\delta)\leqq 1$ one s type localized mode appears in this region under the condition that

$$-\alpha\beta(1+\delta-\beta\delta')-\alpha+1+\delta-\beta\delta'<0\,. \tag{3·11}$$

[When $\delta=\delta'=0$, Eq. (3·11) coincides with Eq. (3·3).] This criterion is illustrated by dotted curves in Fig. 7.*) The localized s modes appear above the boundary curves in the figure. Thus in the present case we have regions where a localized s mode exists in the gap and one more exists below the band. When we fix the values of δ and $\beta\delta'$, this region is much wider than that in which two localized s_0 modes are expected. When $\beta\delta'/(1+\delta)>1$, on the other hand, one s type localized mode appears in the region of $\varepsilon<-1$ if the left-hand side of Eq. (3·11) is smaller than or equal to zero and two s type localized modes appear in the same region if the left-hand side is larger than zero.

Finally we discuss the localized p, d and f modes. These modes cannot be localized in the region, $\varepsilon>1$, as in the case $\delta=\delta'=0$, but can be localized in the region, $\varepsilon<-1$, if $\alpha\beta-1>0$. This criterion for the appearance of these three modes is again the same as that in the case $\delta=\delta'=0$.

§ 4. Application: Mn^{2+} in FeF_2

Here we discuss an application to a real substance of the numerical results obtained in § 3 for the criteria for the appearance of various localized spin-wave modes. Although we have been considering the body-centered cubic lattice, the results may be also applied to the MnF_2 (rutile)-type lattice. This is because we have limited ourselves to the case where there is an exchange interaction between the body-centered and corner sites only; and, in this case, both lattices are topologically equivalent.

We consider the antiferromagnetic crystal FeF_2 in which an Fe^{2+} ion with spin 2 is replaced by an Mn^{2+} ion with spin 5/2. The values of the exchange constant, J, and of the anisotropy constant, D, for FeF_2 can be determined from the neutron diffraction data of Guggenheim, Hutchings and Rainford[9] as follows. They observed that the spin-wave energies at $\boldsymbol{k}=0$ and at the zone boundaries

*) See the second footnote on page 1205.

are 53 and 79 cm^{-1} respectively. Combining these values, $S=2$ and $z=8$ with Eq. (2·9), one calculate the values of J and D for FeF_2 to be 1.8 and 5.2 cm^{-1} respectively. Thus, in the present case, the dimensionless parameters, $\beta(\equiv S'/S)$ and $\delta(\equiv D/Jz)$, are determined to be $\beta=1.25$ and $\delta=0.36$. In order to proceed we assume that the anisotropy constant of the Mn^{2+} ion in FeF_2 is the same as that in pure MnF_2.*) With this value of 0.16 cm^{-1}, which is obtained in our forthcoming paper,[11] the value of $\beta\delta'(\equiv D'S'/JzS)$ becomes 0.014. Unfortunately we do not have at present information enough to determine the exchange integral, J', between the Mn^{2+} and its nearest neighboring intersublattice Fe^{2+} ions. Thus J' is treated as a parameter.

Now we are ready to discuss the Mn^{2+} impurity in FeF_2. As can be seen from Fig. 5, if the Mn^{2+} ion in FeF_2 has a spin which is antiparallel to spins of its nearest neighboring intersublattice Fe^{2+} ions, one localized s_0 mode can be expected above the spin-wave energy band or in the energy gap still on the positive energy side depending on whether $\alpha(\equiv|J'|/J)$ is larger than about 1.3 or smaller than about 1.1. For intermediate values of α, there are no localized s_0 modes. Furthermore we can see from Fig. 9 that one localized s_1 mode will exist below the band if α is larger than about 2. We can expect no localized s_1 mode in the gap, because the value of δ is small. On the other hand, if the direction of the spin associated with the Mn^{2+} ion in FeF_2 is parallel to its nearest neighboring intersublattice Fe^{2+} spins, one s type localized mode is expected below the band for α larger than about 0.5 and another is expected in the gap on the negative energy side for any value of α (see Fig. 7). Finally, one each of the localized p, d and f modes only appear below the band and then only when $\alpha>0.8$. This condition is irrespective of the direction of the Mn^{2+} spin.

The above predictions remain untested as no relevant experimental data have yet been reported.

§ 5. Zero point contraction of spins

(*A*) *Formalism*

Now we turn to the discussion of the zero point contraction of spins caused by a substituted impurity spin in an otherwise pure body-centered cubic antiferromagnet. Only the antiferromagnetic impurity case will be treated.

The ground state expectation values of the z components of spins can be calculated straightforwardly. The results are as follows:

for $j=0$ (impurity),

$$\langle S_0^z\rangle\equiv\langle 0|S'-a_0^*a_0|0\rangle=S'-\sum_\nu|\Gamma_0^\nu|^2, \tag{5·1a}$$

*) This assumption seems to be quite good because the anisotropy energy in MnF_2 comes mainly from the magnetic dipolar interactions between spins.[10] The correction due to the difference between the magnitudes of the magnetic moments of Fe^{2+} and Mn^{2+} ions is negligible in this discussion.

for $j\neq 0$ (host, up sublattice),

$$\langle S_j^z\rangle \equiv \langle 0|S-a_j^*a_j|0\rangle = S-\sum_\nu |\Gamma_j^\nu|^2, \tag{5·1b}$$

and for l (host, down sublattice),

$$\langle S_l^z\rangle \equiv \langle 0|-S+b_l^*b_l|0\rangle = -S+\sum_\mu |\Gamma_l^\mu|^2. \tag{5·1c}$$

Here $|0\rangle$ represents, as before, the ground state wave function of the system. The sums over μ and ν run over the impurity spin-wave modes whose energy eigenvalues are positive and negative respectively. The zero point contraction of up (down) spins comes from the impurity spin-wave modes with negative (positive) energy. In other words, the impurity spin-wave modes contributing to the zero point contraction of a spin are the modes in which the spin precesses unnaturally.*) Hereafter we shall discuss only the zero point contraction of the impurity spin, ΔS_0, and that of its nearest neighbors, ΔS_ρ, which are given by, respectively,

$$\Delta S_0 = \sum_\nu |\Gamma_0^\nu|^2 \tag{5·2a}$$

and

$$\Delta S_\rho = \sum_\mu |\Gamma_\rho^\mu|^2. \tag{5·2b}$$

First consider the zero point contraction of spins resulting from the localized spin-wave modes. Only the localized s_1 mode, if it exists, can contribute to the zero point contraction of the impurity spin. This contribution of the localized s_1 mode, $\Delta S_0^{s_1}$, can be calculated from Eqs. (5·2a) and (2·12a). If we use the dimensionless parameters defined in Eqs. (2·15) and (2·16), the result becomes

$$\begin{aligned}\Delta S_0^{s_1} \equiv |\Gamma_0^{s_1}|^2 = &\frac{(V_0^{s_1})^2}{4S^2(Jz+D)^2} \\ &\times [(1+\delta)v_{s_1} + \{1-(1+\delta)(1-\varepsilon_{s_1})v_{s_1}\}\Gamma(0,0;\delta;\varepsilon_{s_1})]^2\end{aligned} \tag{5·3}$$

with

$$v_{s_1} = V_\rho^{s_1} z / V_0^{s_1}. \tag{5·4}$$

Here we have employed the relation among the Green's functions which is given in the Appendix [see Eq. (A·2d)]. ε_{s_1} is the energy [divided by $2S(Jz+D)$] of the localized s_1 mode which has been discussed in §§ 2 and 3. As $V_\rho^{s_1}$ is independent of ρ (s_1 is an s type mode), v_{s_1} is also independent of ρ. The value of v_{s_1} is calculated from the following equation:

$$\begin{aligned}v_{s_1} = &\frac{(\alpha\beta-1)-\{(\alpha\beta-1)(1-\varepsilon_{s_1})}{(\alpha\beta-1)(1+\delta)(1-\varepsilon_{s_1})-\alpha\sqrt{\beta}-\{(\alpha\beta-1)} \\ &\frac{-(\alpha\sqrt{\beta}-1)/(1+\delta)\}\cdot\Gamma(0,0;\delta;\varepsilon_{s_1})}{\times(1+\delta)(1-\varepsilon_{s_1})-(\alpha\sqrt{\beta}-1)\}\cdot(1-\varepsilon_{s_1})\cdot\Gamma(0,0;\delta;\varepsilon_{s_1})}.\end{aligned} \tag{5·5}$$

*) See reference 5).

Equation (5·5) is obtained from Eq. (5·4) and the equation obtained by summing Eq. (2·13b) over ρ. Furthermore, $[V_0^{s_1}/2S(Jz+D)]^2$ in Eq. (5·3) is calculated from the following equation:

$$\frac{(V_0^{s_1})^2}{4S^2(Jz+D)^2}\cdot[(1+\delta)^2v_{s_1}^2+2(1+\delta)v_{s_1}\{1-(1+\delta)(1-\varepsilon_{s_1})v_{s_1}\}\Gamma(0,0;\delta;\varepsilon_{s_1}) + \{1-(1+\delta)(1-\varepsilon_{s_1})v_{s_1}\}^2\cdot\{\sum_j\Gamma(j,0;\delta;\varepsilon_{s_1}) - \sum_l\Gamma(l,0;\delta;\varepsilon_{s_1})\}] = -1, \tag{5·6}$$

which is obtained from Eqs. (2·12a, b) and the normalization condition for the amplitude of s_1 spin-wave mode.*) In deriving Eqs. (5·5) and (5·6), we used again the relations among the Green's functions [see Eqs. (A·2d) and (A·2f)].

In our discussions we have assumed that the nearest neighboring spins of the impurity spin point in the negative z direction. In this case, only the localized s_0 mode contributes to the zero point contraction of the nearest neighboring spins. (Only when it exists, of course.) We can calculate from Eqs. (2·12b) and (5·2b) the zero point contraction of the nearest neighboring spins, $\Delta S_\rho^{s_0}$, due to the localized s_0 mode as follows:

$$\Delta S_\rho^{s_0}\equiv|\Gamma_\rho^{s_0}|^2=\frac{(V_0^{s_0})^2}{4S^2(Jz+D)^2}(1+\delta)^2\{1-(1+\delta)(1-\varepsilon_{s_0})v_{s_0}\}^2 \times\{1-(1-\varepsilon_{s_0})\Gamma(0,0;\delta;\varepsilon_{s_0})\}^2 \tag{5·7}$$

with

$$v_{s_0}=V_\rho^{s_0}z/V_0^{s_0}, \tag{5·8}$$

where ε_{s_0} is the energy of the localized s_0 mode. Note here that $\Delta S_\rho^{s_0}$ is independent of ρ. v_{s_0} in Eq. (5·7) can be calculated from the expression which is obtained by replacing ε_{s_1} with ε_{s_0} in the right-hand side of Eq. (5·5). Also, $[V_0^{s_0}/2S(Jz+D)]^2$ in Eq. (5·7) can be calculated from the equation obtained by replacing $V_0^{s_1}$ with $V_0^{s_0}$, ε_{s_1} with ε_{s_0} and v_{s_1} with v_{s_0} in Eq. (5·6) and changing the right-hand side of the resulting equation to $+1$.

Next we consider the zero point contraction of the impurity spin and its nearest neighbors resulting from the impurity spin-wave modes whose energies are inside the energy continuum. In this case it is not convenient to apply the method which was used in the discussion of the zero point contraction of spins due to the localized modes. Therefore we use here the following method which employs a scattering approach. In this method we determine the energies of the impurity spin-wave modes beforehand and then calculate the coefficients, Γ_j^λ

*) The normalization condition $\sum_j|\Gamma_j^{s_1}|^2-\sum_l|\Gamma_l^{s_1}|^2=-1$ is equivalent to the commutation relation $[c_{s_1}^*, c_{s_1}]=1$.

and Γ_l^{λ}. The corresponding method has been developed by Koster and Slater[12] in their studies of the impurity problem of electrons in solids.

The coefficients, $\Gamma_j^{k\tau}$ and $\Gamma_l^{k\tau}$, associated with the impurity spin-wave modes whose energy eigenvalues are $E_{k\tau}^{(0)}$ ($\tau=+$ or $-$), defined by Eq. (2·9), may be written as follows:

$$\Gamma_j^{k\tau}=\frac{1}{\sqrt{N}}p_{k\tau}e^{ik\cdot R_j}+V_0^{k\tau}G(j,\,0;\,E_{k\tau}^{(0)+})+\sum_{\rho}V_{\rho}^{k\tau}G(j,\,\rho;\,E_{k\tau}^{(0)+}), \tag{5·9a}$$

$$\Gamma_l^{k\tau}=\frac{1}{\sqrt{N}}q_{k\tau}e^{ik\cdot R_l}+V_0^{k\tau}G(l,\,0;\,E_{k\tau}^{(0)+})+\sum_{\rho}V_{\rho}^{k\tau}G(l,\,\rho;\,E_{k\tau}^{(0)+}), \tag{5·9b}$$

where $E_{k\tau}^{(0)+}=E_{k\tau}^{(0)}+i\eta$ $(\eta=0_+)$. $p_{k\tau}$ and $q_{k\tau}$ are defined by Eqs. (2·10a) and (2·10b) respectively. When E_λ assumes the value $E_{k\tau}^{(0)}$, Eqs. (2·6b, d) are automatically satisfied by these $\Gamma_j^{k\tau}$ and $\Gamma_l^{k\tau}$. Furthermore, by substituting Eqs. (5·9a, b) into Eqs. (2·6a, c) and taking $E_\lambda=E_{k\tau}^{(0)}$, $V_0^{k\tau}$ and $V_\rho^{k\tau}$ can be expressed in terms of $\Gamma_0^{k\tau}$ and $\Gamma_\rho^{k\tau}$. Substituting next the $V_0^{k\tau}$ and $V_\rho^{k\tau}$ thus obtained into Eqs. (5·9a, b), we can express $\Gamma_j^{k\tau}$ and $\Gamma_l^{k\tau}$ in terms of $\Gamma_0^{k\tau}$ and $\Gamma_\rho^{k\tau}$. Finally, from these equations the following set of simultaneous equations, which determines $\Gamma_0^{k\tau}$ and $\Gamma_\rho^{k\tau}$, is obtained:

$$\begin{aligned}\frac{1}{\sqrt{N}}p_{k\tau}=\Gamma_0^{k\tau}&[1+\{2(J'-J)Sz+2(D'S'-DS)\}G(0,\,0;\,E_{k\tau}^{(0)+})\\&+2(J'\sqrt{SS'}-JS)\sum_{\rho'}G(0,\,\rho';\,E_{k\tau}^{(0)+})]\\+\sum_{\rho'}\Gamma_{\rho'}^{k\tau}&[-2(J'\sqrt{SS'}-JS)G(0,\,0;\,E_{k\tau}^{(0)+})\\&-2(J'S'-JS)G(0,\,\rho';\,E_{k\tau}^{(0)+})],\end{aligned} \tag{5·10a}$$

$$\begin{aligned}\frac{1}{\sqrt{N}}q_{k\tau}e^{ik\cdot R_\rho}=\Gamma_0^{k\tau}&[\{2(J'-J)Sz+2(D'S'-DS)\}G(\rho,\,0;\,E_{k\tau}^{(0)+})\\&+2(J'\sqrt{SS'}-JS)\sum_{\rho'}G(\rho,\,\rho';\,E_{k\tau}^{(0)+})]\\+\sum_{\rho'}\Gamma_{\rho'}^{k\tau}&[\delta_{\rho,\rho'}-2(J'\sqrt{SS'}-JS)G(\rho,\,0;\,E_{k\tau}^{(0)+})\\&-2(J'S'-JS)G(\rho,\,\rho';\,E_{k\tau}^{(0)+})].\end{aligned} \tag{5·10b}$$

Using the symmetry properties of the Green's functions, we can solve these simultaneous equations. The results for the case of body-centered cubic lattice are

$$\Gamma_0^{k\tau}=\frac{1}{D_s^{AF}(\varepsilon_{k\tau}^{(0)+})}\cdot\frac{J'\sqrt{SS'}}{JS}\cdot\frac{1}{\sqrt{N}}p_{k\tau} \tag{5·11a}$$

and

$$\begin{aligned}\Gamma_{\rho}^{k\tau}=&\frac{1}{D_s^{AF}(\varepsilon_{k\tau}^{(0)+})}\cdot\left[\frac{J'}{J}+\frac{D'S'}{JzS}-\frac{E_{k\tau}^{(0)}}{2JSz}\right]\cdot\frac{1}{\sqrt{N}}p_{k\tau}\\&+\frac{1}{z}\cdot\frac{1}{D_p(\varepsilon_{k\tau}^{(0)+})}\cdot\frac{1}{\sqrt{N}}q_{k\tau}\cdot\{4(e^{ik\cdot R_\rho}-e^{-ik\cdot R_\rho})\mp(\gamma_k^{(1)}-\gamma_k^{(2)})\}\\&+\frac{1}{z}\cdot\frac{1}{D_d(\varepsilon_{k\tau}^{(0)+})}\cdot\frac{1}{\sqrt{N}}q_{k\tau}\cdot\{4(e^{ik\cdot R_\rho}+e^{-ik\cdot R_\rho})-\gamma_k\}\qquad(5\cdot11\text{b})\\&\pm\frac{1}{z}\cdot\frac{1}{D_f(\varepsilon_{k\tau}^{(0)+})}\cdot\frac{1}{\sqrt{N}}q_{k\tau}\cdot\{\gamma_k^{(1)}-\gamma_k^{(2)}\},\end{aligned}$$

where

$$\varepsilon_{k\tau}^{(0)+}=E_{k\tau}^{(0)+}/2S(Jz+D),\qquad(5\cdot12)$$

$$\gamma_k^{(1)}=e^{ik\cdot R_{111}}+e^{ik\cdot R_{1-1-1}}+e^{ik\cdot R_{-11-1}}+e^{ik\cdot R_{-1-11}},$$

$$\gamma_k^{(2)}=e^{ik\cdot R_{-111}}+e^{ik\cdot R_{1-11}}+e^{ik\cdot R_{11-1}}+e^{ik\cdot R_{-1-1-1}}.\qquad(5\cdot13)$$

$D_s^{AF}(\varepsilon)$, $D_p(\varepsilon)$, $D_d(\varepsilon)$, $D_f(\varepsilon)$ and γ_k have already been defined by Eqs. (2·14), (2·19), (2·20), (2·21) and (2·11), respectively. If R_ρ is one of the four nearest neighboring vectors, R_{111}, R_{1-1-1}, R_{-11-1} and R_{-1-11}, then we take the upper sign in Eq. (5·11b). On the other hand, if R_ρ is one of the other four nearest neighboring vectors (R_{-111}, R_{1-11}, R_{11-1} and R_{-1-1-1}), then the lower sign applies. $\Gamma_j^{k\tau}$ ($j\neq0$) and $\Gamma_l^{k\tau}$ ($l\neq\rho$) are calculated by substituting the values for $\Gamma_0^{k\tau}$ and $\Gamma_\rho^{k\tau}$ from Eqs. (5·11a, b) into equations (not given explicitly) which express $\Gamma_j^{k\tau}$ and $\Gamma_l^{k\tau}$ in terms of $\Gamma_0^{k\tau}$ and $\Gamma_\rho^{k\tau}$.

Now we are ready to calculate the zero point contraction of the impurity spin, ΔS_0^{cont}, and that of its nearest neighbors, $\Delta S_\rho^{\text{cont}}$, resulting from the impurity spin-wave modes whose energies are inside the energy continuum. From Eqs. (5·2a) and (5·11a), ΔS_0^{cont} becomes

$$\Delta S_0^{\text{cont}}\equiv\sum_k|\Gamma_0^{k-}|^2=-\frac{\alpha^2\beta}{\pi}\int_{-1}^{0}d\varepsilon\,\frac{\text{Im}[\Gamma(0,0;\delta;\varepsilon+i\eta)]}{|D_s^{AF}(\varepsilon+i\eta)|^2},\qquad(5\cdot14)$$

and similarly from Eqs. (5·2b) and (5·11b) we get for $\Delta S_\rho^{\text{cont}}$

$$\begin{aligned}\Delta S_\rho^{\text{cont}}\equiv&\sum_k|\Gamma_\rho^{k+}|^2\\=&\frac{1}{\pi}\left[\int_0^1d\varepsilon\{\alpha+\beta\delta'-(1+\delta)\varepsilon\}^2\cdot\frac{\text{Im}[\Gamma(0,0;\delta;\varepsilon+i\eta)]}{|D_s^{AF}(\varepsilon+i\eta)|^2}\right.\\&-\frac{3}{z}\int_0^1\frac{d\varepsilon}{|D_p(\varepsilon+i\eta)|^2}\cdot\text{Im}\{\Gamma(111,111;\delta;\varepsilon+i\eta)+\Gamma(111,11-1;\delta;\varepsilon+i\eta)\\&\left.-\Gamma(111,1-1-1;\delta;\varepsilon+i\eta)-\Gamma(111,-1-1-1;\delta;\varepsilon+i\eta)\}\right.\end{aligned}$$

$$-\frac{3}{z}\int_0^1 \frac{d\varepsilon}{|D_a(\varepsilon+i\eta)|^2}\cdot \mathrm{Im}\{\Gamma(111,\,111;\,\delta;\,\varepsilon+i\eta)-\Gamma(111,\,11-1;\,\delta;\,\varepsilon+i\eta)$$

$$-\Gamma(111,\,1-1-1;\,\delta;\,\varepsilon+i\eta)+\Gamma(111,\,-1-1-1;\,\delta;\,\varepsilon+i\eta)\}$$

$$-\frac{1}{z}\int_0^1 \frac{d\varepsilon}{|D_f(\varepsilon+i\eta)|^2}\cdot \mathrm{Im}\{\Gamma(111,\,111;\,\delta;\,\varepsilon+i\eta)-3\Gamma(111,\,11-1;\,\delta;\,\varepsilon+i\eta)$$

$$+3\Gamma(111,\,1-1-1;\,\delta;\,\varepsilon+i\eta)-\Gamma(111,\,-1-1-1;\,\delta;\,\varepsilon+i\eta)\}\Big]. \tag{5·15}$$

Here we used the cubic symmetry properties of the lattice. The $\Delta S_\rho^{\mathrm{cont}}$ thus obtained are, of course, independent of ρ.

Finally, the total zero point contraction of the impurity spin, ΔS_0, and that of its nearest neighbors, ΔS_ρ, are expressed as

$$\Delta S_0=\Delta S_0^{\mathrm{cont}}+\Delta S_0^{s_1} \tag{5·16a}$$

and

$$\Delta S_\rho=\Delta S_\rho^{\mathrm{cont}}+\Delta S_\rho^{s_0}, \tag{5·16b}$$

respectively, in the antiferromagnetic impurity case. $\Delta S_0^{s_1}$, $\Delta S_\rho^{s_0}$, $\Delta S_0^{\mathrm{cont}}$ and $\Delta S_\rho^{\mathrm{cont}}$ in Eqs. (5·16a, b) are given by Eqs. (5·3), (5·7), (5·14) and (5·15), respectively. Of course, the former two quantities contribute to the zero point contraction of each spin only when the corresponding localized spin-wave modes exist. We can easily show that, when $\alpha=\beta=1$ and $\delta'=\delta$ (pure antiferromagnet case), the above obtained ΔS_0 and ΔS_ρ become identical and they agree with the expression for the zero point spin contraction in pure antiferromagnets, ΔS_{pure}, obtained by Anderson[13] and also by Kubo[14] in the linear spin-wave approximation. In our notation ΔS_{pure} is given as follows:

$$\Delta S_{\mathrm{pure}}=-\frac{1}{2}\left[1-\frac{1}{N}\sum_{\boldsymbol{k}}\frac{1+\delta}{\sqrt{(1+\delta)^2-(\gamma_{\boldsymbol{k}}/z)^2}}\right], \tag{5·17}$$

where the summation with respect to $\boldsymbol{k}$ is taken over the first Brillouin zone.

(B) Numerical calculations and discussion

Figure 10 indicates the result of the numerical calculation of the zero point contraction of the impurity spin, ΔS_0, in a body-centered cubic antiferromagnet with an antiferromagnetically coupled impurity for the case of $\delta=\delta'=0$. In the figure, ΔS_0 for various values of α are given as a function of β. The corresponding result for the nearest neighboring spins is shown in Fig. 11. Here we considered only the cases in which there are no localized spin-wave modes. The numerical integrations for $\Delta S_0^{\mathrm{cont}}$ and $\Delta S_\rho^{\mathrm{cont}}$ were carried out on the NEAC 2200 electronic computer using Simpson's method.

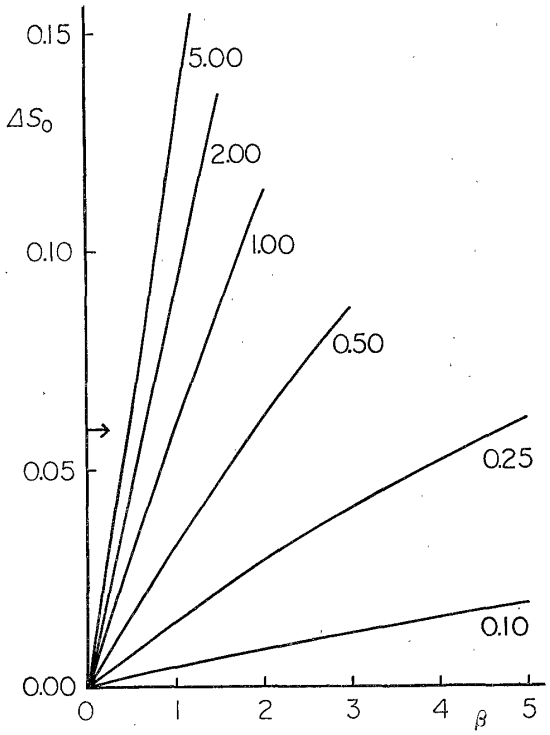

Fig. 10. Calculated zero point contraction of the impurity spin in a body-centered cubic antiferromagnet with an antiferromagnetically coupled impurity for the case $\delta=\delta'=0$. The contraction is shown as a function of β for various α. Numerical figures denote the values of α. The value of the contraction in a pure body-centered cubic antiferromagnet, 0.0593, is marked by an arrow.

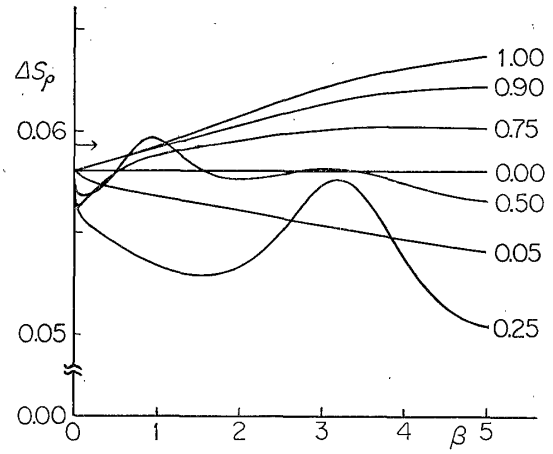

Fig. 11. Same as Fig. 10 for the nearest neighboring spins of the impurity.

In particular the calculated value of ΔS_0 and ΔS_ρ for the $\alpha=\beta=1$ case (pure antiferromagnet case), which were denoted by ΔS_{pure} in the preceding subsection, is 0.0593. This value does not coincide with that obtained by Kubo[14] for the body-centered cubic lattice. This is because Kubo's numerical integration of the right-hand side of Eq. (5·17) is wrong. Kubo has calculated the same integral in another paper[15] and obtained the value of 0.0593, with which our result agrees. We note here that the zero point contractions of the impurity spin and its nearest neighbors which come from the impurity effect are given by $\Delta S_0-\Delta S_{\text{pure}}$ and $\Delta S_\rho-\Delta S_{\text{pure}}$, respectively.

As seen from Fig. 11, the zero point contraction of the nearest neighboring spins of the impurity has an oscillating property as a function of β and also as a function of α. Another point of interest is that, although it might seem strange at first glance, the zero point contraction of the nearest neighboring spins actually decreases as β increases from zero for sufficiently small α. This situation, however, can be expected also in the result obtained from the simple perturbation calculation. This result is given by $[\alpha^2\beta/(z-1+\alpha\beta+z\alpha)^2]+[(z-1)/(2z-1+\alpha\beta)^2]$, where $z=8$. The initial derivative of the above quantity with respect to β is negative when α is less than about 0.5. Thus our result in the linear spin-wave approximation seems to be quite reasonable.

§ 6. Concluding remarks

We have developed in the linear spin-wave approximation a theory for the spin-wave impurity problem in an antiferromagnet containing a single impurity spin. We have considered a simple Heisenberg spin Hamiltonian with an intersublattice exchange interaction only, plus an anisotropy energy term of the form of $-DS_z^2$; both the cases of antiferromagnetic and ferromagnetic coupling between the impurity and its nearest neighboring host spins have been investigated. In the numerical calculations we have confined ourselves to the bodycentered cubic and MnF_2 (rutile)-type lattices, which are topologically equivalent to each other in the present case. In these lattices the impurity spin-wave modes can be classified into s, p, d and f modes. Both the conditions under which the modes are localized and the energies of the modes so obtained have been examined for various combinations of the four parameters, $\alpha(=|J'|/J)$, $\beta(=S'/S)$, $\delta(=D/Jz)$ and $\delta'(=D'/Jz)$.

The results regarding the criteria for the appearance of various types of localized modes have been applied to discuss an Mn^{2+} impurity in the antiferromagnetic crystal FeF_2. It has been shown that, if the Mn^{2+} spin is antiparallel to its nearest neighboring intersublattice Fe^{2+} spins, one each of the localized s_0, s_1, p, d and f modes can be expected. The localized s_0 mode appears either above the spin-wave energy band or in the energy gap still on the positive energy side depending upon whether α is larger than about 1.3 or smaller than about 1.1. For intermediate values of α, there are no localized s_0 modes. When α is larger than about 2, a localized s_1 mode occurs; it appears below the band. When $\alpha>0.8$, one each of the localized p, d and f modes appear, also below the band.

On the other hand, if the Mn^{2+} spin in FeF_2 is parallel to its nearest neighboring intersublattice Fe^{2+} spins, we can expect one s type localized mode below the band for α larger than about 0.5 and another s type mode in the gap on the negative energy side for any value of α. We can also expect one each of the localized p, d and f modes below the band when α is larger than 0.8, since the appearance of these modes is independent of the direction of the Mn^{2+} spin.

Finally the zero point contraction of the impurity and its nearest neighboring spins in a body-centered cubic antiferromagnet with an antiferromagnetically coupled impurity has been discussed. Numerical results have been given for various cases in which both δ and δ' are set equal to zero and values of α and β are chosen in such a manner that there are no localized spin-wave modes. It has been found that the zero point contraction of the nearest neighboring spins is an oscillating function of α and β.

Acknowledgments

The author would like to express his sincere thanks to Professor J. Kanamori for suggesting the present problem and for continued encouragement and

advice throughout the course of this study. He would like to thank Dr. R. S. Alben for correcting the manuscript. Thanks are also due to Mr. H. Ishii for discussions in the earlier part of this study. The present work has been supported in part by a Grant in Aid from the Education Ministry.

Appendix

Green's functions for a body-centered cubic lattice

(A) *Analytical forms of the Green's functions*

For a body-centered cubic lattice with a nearest neighboring intersublattice exchange interaction, the analytical forms of the dimensionless Green's functions defined by Eq. (2·17) are deduced as follows:

$$\Gamma(j, j'; \delta;\varepsilon) = (1+\delta)^2(\varepsilon+1)\frac{8}{\pi^3} \times \int_0^{\pi/2}\!\!\int\!\!\int \frac{\cos[(n_x-n_x')x]\cdot\cos[(n_y-n_y')y]\cdot\cos[(n_z-n_z')z]}{(1+\delta)^2(1-\varepsilon^2)-\cos^2x\cdot\cos^2y\cdot\cos^2z}\,dxdydz\,, \quad (|n_i|,\ |n_i'|\ \ (i=x, y, z)\text{: even}) \tag{A·1a}$$

$$\Gamma(j, l'; \delta; \varepsilon) = -(1+\delta)\frac{8}{\pi^3} \times \int_0^{\pi/2}\!\!\int\!\!\int \cos[(n_x-n_x')x]\cdot\cos[(n_y-n_y')y]\cdot\cos[(n_z-n_z')z] \times \frac{\cos x\cdot\cos y\cdot\cos z}{(1+\delta)^2(1-\varepsilon^2)-\cos^2x\cdot\cos^2y\cdot\cos^2z}\,dxdydz\,, \quad (|n_i|\text{: even},\ |n_i'|\text{: odd}) \tag{A·1b}$$

$$\Gamma(l, j'; \delta; \varepsilon) = (1+\delta)\frac{8}{\pi^3} \times \int_0^{\pi/2}\!\!\int\!\!\int \cos[(n_x-n_x')x]\cdot\cos[(n_y-n_y')y]\cdot\cos[(n_z-n_z')z] \times \frac{\cos x\cdot\cos y\cdot\cos z}{(1+\delta)^2(1-\varepsilon^2)-\cos^2x\cdot\cos^2y\cdot\cos^2z}\,dxdydz\,, \quad (|n_i|\text{: odd},\ |n_i'|\text{: even}) \tag{A·1c}$$

$$\Gamma(l, l'; \delta; \varepsilon)$$
$$= (1+\delta)^2(\varepsilon-1)\frac{8}{\pi^3}$$
$$\times\int_0^{\pi/2}\int\int\frac{\cos[(n_x-n_x')x]\cdot\cos[(n_y-n_y')y]\cdot\cos[(n_z-n_z')z]}{(1+\delta)^2(1-\varepsilon^2)-\cos^2x\cdot\cos^2y\cdot\cos^2z}\,dxdydz\,.$$
$$(|n_i|,\ |n_i'|:\ \text{odd}) \qquad (A\cdot 1d)$$

Here we have employed the dimensionless parameters defined by Eqs. (2·15) and (2·16). $\boldsymbol{R}_j$ and $\boldsymbol{R}_l$ have been taken as the vectors $(n_xa/2, n_ya/2, n_za/2)$ with even $|n_i|$ and odd $|n_i|$, respectively. (a is the lattice constant.) In deriving Eqs. (A·1a, b, c, d), the cubic symmetry of the lattice was used.

(B) *Relations among the Green's functions*

From Eqs. (A·1a, b, c, d) we can obtain relations among the Green's functions. These relations are, for example:

$$(\varepsilon-1)\Gamma(j, j'; \delta; \varepsilon) = (\varepsilon+1)\Gamma(j+l, j'+l; \delta; \varepsilon), \qquad (A\cdot 2a)$$

$$\Gamma(j, j'; \delta; -\varepsilon) = \frac{1-\varepsilon}{1+\varepsilon}\Gamma(j, j'; \delta; \varepsilon), \qquad (A\cdot 2b)$$

$$\frac{1}{z}\sum_\rho\Gamma(j, \rho; \delta; \varepsilon) = -\frac{1}{z}\sum_\rho\Gamma(\rho, j; \delta; \varepsilon) \qquad (A\cdot 2c)$$
$$= (1+\delta)\delta_{j,0} - (1+\delta)(1-\varepsilon)\Gamma(j, 0; \delta; \varepsilon), \qquad (A\cdot 2d)$$

$$\frac{1}{z^2}\sum_{\rho,\rho'}\Gamma(j+\rho, \rho'; \delta; \varepsilon)$$
$$= (1+\delta)^2(1-\varepsilon)\delta_{j,0} - (1+\delta)^2(1-\varepsilon)^2\Gamma(j, 0; \delta; \varepsilon), \qquad (A\cdot 2e)$$

$$\frac{1}{z}\sum_\rho\Gamma(l, \rho; \delta; \varepsilon) = -(1+\delta)(1-\varepsilon)\Gamma(l, 0; \delta; \varepsilon). \qquad (A\cdot 2f)$$

We note here that the vector $\boldsymbol{R}_j$ is associated with the lattice point with positive spin, and the vectors $\boldsymbol{R}_l$, $\boldsymbol{R}_\rho$, $\boldsymbol{R}_{j+l}$ and $\boldsymbol{R}_{j+\rho}$ are associated with the lattice points with negative spin.

As $\Gamma(\rho, 0; \delta; \varepsilon)$, $\Gamma(0, \rho; \delta; \varepsilon)$ and $(1/z)\sum_{\rho'}\Gamma(\rho, \rho'; \delta; \varepsilon)$ are independent of the direction of $\boldsymbol{R}_\rho$, these Green's functions are expressed from Eqs. (A·2c, d, e) as follows:

$$\Gamma(0, \rho; \delta; \varepsilon) = -\Gamma(\rho, 0; \delta; \varepsilon)$$
$$= (1+\delta) - (1+\delta)(1-\varepsilon)\Gamma(0, 0; \delta; \varepsilon), \qquad (A\cdot 3a)$$

$$\frac{1}{z}\sum_{\rho'}\Gamma(\rho, \rho'; \delta; \varepsilon)$$
$$= (1+\delta)^2(1-\varepsilon) - (1+\delta)^2(1-\varepsilon)^2\Gamma(0, 0; \delta; \varepsilon). \qquad (A\cdot 3b)$$

The relations obtained above were used in the text. Note that we can use the above mentioned relations as well as others (not given here) to check the accuracy of any numerical evaluation of the Green's functions.

(C) *Method of calculation of the Green's functions*

Here we discuss the method of numerical calculation of the Green's functions, $\Gamma(j, j'; \delta; \varepsilon+i\eta)$, $\Gamma(j, l'; \delta; \varepsilon+i\eta)$, $\Gamma(l, j'; \delta; \varepsilon+i\eta)$ and $\Gamma(l, l'; \delta; \varepsilon+i\eta)$, where $\eta=0_+$. When the energy ε is outside the spin-wave energy continuum [$|\varepsilon|>1$ or $|\varepsilon|<\sqrt{2\delta+\delta^2}/(1+\delta)$], the denominators of the integrands in Eqs. (A·1 a, b, c, d) are never zero. Thus, in this case, the values of the four Green's functions mentioned above are equal to those of $\Gamma(j, j'; \delta; \varepsilon)$, $\Gamma(j, l'; \delta; \varepsilon)$, $\Gamma(l, j'; \delta; \varepsilon)$ and $\Gamma(l, l'; \delta; \varepsilon)$, respectively. These can be calculated by numerical integration.

In performing these operations for the special case of $\Gamma(0, 0; \delta; \varepsilon)$ and $\Gamma(\rho, \rho'; \delta; \varepsilon)$ for energy outside the continuum, it is convenient to rewrite these Green's functions as follows:*)

$$\Gamma(0, 0; \delta; \varepsilon) = -(1+\delta)^2(\varepsilon+1)\cdot f_0((1+\delta)^2(\varepsilon^2-1)), \tag{A·4a}$$

$$\Gamma(111, 111; \delta; \varepsilon) = -(1+\delta)^2(\varepsilon-1)\cdot f_0((1+\delta)^2(\varepsilon^2-1)), \tag{A·4b}$$

$$\Gamma(111, 11-1; \delta; \varepsilon) = -(1+\delta)^2(\varepsilon-1)\cdot\{2f_1((1+\delta)^2(\varepsilon^2-1)) - f_0((1+\delta)^2(\varepsilon^2-1))\}, \tag{A·4c}$$

$$\Gamma(111, 1-1-1; \delta; \varepsilon) = -(1+\delta)^2(\varepsilon-1)\cdot\{4f_2((1+\delta)^2(\varepsilon^2-1)) - 4f_1((1+\delta)^2(\varepsilon^2-1)) + f_0((1+\delta)^2(\varepsilon^2-1))\}, \tag{A·4d}$$

$$\Gamma(111, -1-1-1; \delta; \varepsilon) = -(1+\delta)^2(\varepsilon-1)\cdot[8-12f_2((1+\delta)^2(\varepsilon^2-1)) + 6f_1((1+\delta)^2(\varepsilon^2-1)) - \{1+8(1+\delta)^2(\varepsilon^2-1)\}\cdot f_0((1+\delta)^2(\varepsilon^2-1))], \tag{A·4e}$$

where

$$f_0(t) = \frac{8}{\pi^3}\int_0^{\pi/2}\!\!\int\!\!\int \frac{1}{t+\cos^2x\cdot\cos^2y\cdot\cos^2z}\,dxdydz, \tag{A·5a}$$

$$f_1(t) = \frac{8}{\pi^3}\int_0^{\pi/2}\!\!\int\!\!\int \frac{\cos^2z}{t+\cos^2x\cdot\cos^2y\cdot\cos^2z}\,dxdydz, \tag{A·5b}$$

$$f_2(t) = \frac{8}{\pi^3}\int_0^{\pi/2}\!\!\int\!\!\int \frac{\cos^2y\cdot\cos^2z}{t+\cos^2x\cdot\cos^2y\cdot\cos^2z}\,dxdydz. \tag{A·5c}$$

The reason is that, if we know the values of $f_0(t)$, $f_1(t)$ and $f_2(t)$ for $t>0$ or

*) Note that $\Gamma(\rho, \rho'; \delta; \varepsilon)$ depends only on $|\boldsymbol{R}_\rho-\boldsymbol{R}_{\rho'}|$.

$t<-1$, then we can calculate $\Gamma(0, 0; \delta; \varepsilon)$ and $\Gamma(\rho, \rho'; \delta; \varepsilon)$ for any set of δ such that $\delta \geqq 0$ and ε such that $|\varepsilon|>1$ or $|\varepsilon|<\sqrt{2\delta+\delta^2}/(1+\delta)$.

By integrating with respect to x in Eqs. (A·5a, b, c), the triplet integrals are reduced to single integrals as follows:

$$f_0(t)=\begin{cases}\dfrac{4}{\pi^2}\dfrac{1}{\sqrt{t}}\displaystyle\int_0^{\pi/2}\frac{1}{\sqrt{t+\cos^2 z}}\cdot F\left(\frac{\pi}{2}, \frac{\cos z}{\sqrt{t+\cos^2 z}}\right)dz, & \text{for } t>0, \quad (A\cdot 6a)\\ \dfrac{4}{\pi^2}\dfrac{1}{t}\displaystyle\int_0^{\pi/2} F\left(\frac{\pi}{2}, \frac{\cos z}{\sqrt{-t}}\right)dz, & \text{for } t<-1, \quad (A\cdot 6b)\end{cases}$$

$$f_1(t)=\begin{cases}\dfrac{4}{\pi^2}\dfrac{1}{\sqrt{t}}\displaystyle\int_0^{\pi/2}\frac{\cos^2 z}{\sqrt{t+\cos^2 z}}\cdot F\left(\frac{\pi}{2}, \frac{\cos z}{\sqrt{t+\cos^2 z}}\right)dz, & \text{for } t>0, \quad (A\cdot 7a)\\ \dfrac{4}{\pi^2}\dfrac{1}{t}\displaystyle\int_0^{\pi/2}\cos^2 z\cdot F\left(\frac{\pi}{2}, \frac{\cos z}{\sqrt{-t}}\right)dz, & \text{for } t<-1, \quad (A\cdot 7b)\end{cases}$$

$$f_2(t)=\begin{cases}\dfrac{4}{\pi^2}\dfrac{1}{\sqrt{t}}\displaystyle\int_0^{\pi/2}\left\{\sqrt{t+\cos^2 z}\cdot E\left(\frac{\pi}{2}, \frac{\cos z}{\sqrt{t+\cos^2 z}}\right)\right. & \\ \qquad\left.-\dfrac{t}{\sqrt{t+\cos^2 z}}\cdot F\left(\frac{\pi}{2}, \frac{\cos z}{\sqrt{t+\cos^2 z}}\right)\right\}dz, & \text{for } t>0, \quad (A\cdot 8a)\\ \dfrac{4}{\pi^2}\displaystyle\int_0^{\pi/2}\left\{E\left(\frac{\pi}{2}, \frac{\cos z}{\sqrt{-t}}\right)-F\left(\frac{\pi}{2}, \frac{\cos z}{\sqrt{-t}}\right)\right\}dz, & \text{for } t<-1, \quad (A\cdot 8b)\end{cases}$$

where $F(\pi/2, \kappa)$ and $E(\pi/2, \kappa)$ are the elliptic integrals of the first and second kinds, respectively. The values of $f_0(t)$ for $t>0$ and $t<-1$ and those of $f_1(t)$ and $f_2(t)$ for $t>0$ have been calculated by Simpson's rule with an interval of $\pi/20$; the results are tabulated in Table I. Combining these values with Eqs. (A·4a, b, c, d, e), we can calculate the values of $\Gamma(0, 0; \delta; \varepsilon)$ for ε and δ in the regions, $|\varepsilon|>1$ and $\delta \geqq 0$, and $|\varepsilon|<\sqrt{2\delta+\delta^2}/(1+\delta)$ and $\delta \geqq 0$, and also the values of $\Gamma(111, 111; \delta; \varepsilon)$, $\Gamma(111, 11-1; \delta; \varepsilon)$, $\Gamma(111, 1-1-1; \delta; \varepsilon)$ and $\Gamma(111, -1-1-1; \delta; \varepsilon)$ for $|\varepsilon|>1$ and $\delta \geqq 0$. These values were used in the text to calculate the energies of the various types of localized modes.

On the other hand, when the energy, ε, is inside the spin-wave energy continuum $[1>|\varepsilon|>\sqrt{2\delta+\delta^2}/(1+\delta)]$, the Green's functions are calculated by the following different method. First define $f(x)$ and $g(x)$ to be arbitrary regular functions subject only to the condition that $f(x)=0$ always has only one solution (non-degenerate), x_0, in the region $0<x_0<a$, and consider the following integral:

Table I. Numerical values of the functions, $f_0(t)$, $f_1(t)$ and $f_2(t)$. These are defined by Eqs. (A·5a), (A·5b) and (A·5c), respectively.

Table IA. Numerical values of $f_0(t)$, $f_1(t)$ and $f_2(t)$ for $t>0$.

t	$f_0(t)$	$f_1(t)$	$f_2(t)$
24.00	0.041453	0.020674	0.010297
19.25	0.051618	0.025727	0.012802
15.00	0.066126	0.032929	0.016365
11.25	0.087936	0.043733	0.021691
8.00	0.12314	0.061115	0.030218
5.25	0.18627	0.092109	0.045294
3.00	0.32109	0.15761	0.076643
1.89	0.50014	0.24327	0.11668
1.25	0.73877	0.35537	0.16758
1.00	0.90917	0.43416	0.20246
0.80	1.11630	0.52866	0.24341
0.60	1.44915	0.67798	0.30635
0.45	1.87321	0.86432	0.38225
0.30	2.66973	1.20476	0.51466
0.20	3.77208	1.66011	0.68180
0.10	6.68214	2.80338	1.06703

Table IB. Numerical values of $f_0(t)$ for $t<-1$.

t	$f_0(t)$	t	$f_0(t)$
−1.1	−1.12042	−2.6	−0.40702
−1.2	−0.98929	−2.7	−0.39097
−1.3	−0.89157	−2.8	−0.37615
−1.4	−0.81367	−2.9	−0.36242
−1.5	−0.74937	−3.0	−0.34966
−1.6	−0.69508	−3.1	−0.33778
−1.7	−0.64847	−3.2	−0.32669
−1.8	−0.60795	−3.3	−0.31630
−1.9	−0.57234	−3.4	−0.30656
−2.0	−0.54077	−3.5	−0.29740
−2.1	−0.51258	−3.6	−0.28878
−2.2	−0.48723	−3.7	−0.28064
−2.3	−0.46431	−3.8	−0.27295
−2.4	−0.44348	−3.9	−0.26568
−2.5	−0.42445	−4.0	−0.25878

$$I=\int_0^a \frac{g(x)}{f(x)-i\eta}\,dx\,. \tag{A·9}$$

Using a well-known relation, $1/(x-i\eta)=\mathcal{P}(1/x)+i\pi\delta(x)$, we get

Table II. Representative values of the Green's functions, $\Gamma(000, 000; \delta; \varepsilon+i\eta)$, $\Gamma(002, 000; \delta; \varepsilon+i\eta)$, $\Gamma(022, 000; \delta; \varepsilon+i\eta)$ and $\Gamma(222, 000; \delta; \varepsilon+i\eta)$ [see Eq. (A·1a)], for $1>\varepsilon\geqq\sqrt{2\delta+\delta^2}/(1+\delta)$ in the case of $\delta=0$ (note, $\eta=0_+$). Those for $-1<\varepsilon\leqq-\sqrt{2\delta+\delta^2}/(1+\delta)$ are easily obtained by using Eq. (A·2b). Also the Green's functions, $\Gamma(111, 111; \delta; \varepsilon+i\eta)$, $\Gamma(111, 11-1; \delta; \varepsilon+i\eta)$, $\Gamma(111, 1-1-1; \delta; \varepsilon+i\eta)$ and $\Gamma(111, -1-1-1; \delta; \varepsilon+i\eta)$ [see Eq. (A·1d)], for $\delta=0$ are obtained from Eq. (A·2a) and the values listed below. More complete tables are available upon request.

Table IIA. Real parts.

ε	$\mathrm{Re}[\Gamma(000, 000; 0; \varepsilon+i\eta)]$	$\mathrm{Re}[\Gamma(002, 000; 0; \varepsilon+i\eta)]$	$\mathrm{Re}[\Gamma(022, 000; 0; \varepsilon+i\eta)]$	$\mathrm{Re}[\Gamma(222, 000; 0; \varepsilon+i\eta)]$
0.99	36.155	−17.955	1.0243	4.4091
0.97	18.046	−7.3544	−1.4974	1.2784
0.95	12.949	−4.5611	−1.6755	0.26853
0.90	8.1578	−2.0886	−1.3854	−0.52005
0.85	6.1761	−1.1439	−1.0503	−0.66412
0.80	5.0460	−0.64275	−0.77683	−0.63539
0.70	3.7635	−0.13221	−0.38267	−0.44428
0.60	3.0323	0.10991	−0.12608	−0.23932
0.50	2.5486	0.23552	0.04167	−0.07051
0.40	2.1993	0.29942	0.14818	0.05411
0.20	1.7180	0.32977	0.23954	0.18341
0.00	1.3915	0.29222	0.22864	0.19062

Table IIB. Imaginary parts.

ε	$\mathrm{Im}[\Gamma(000, 000; 0; \varepsilon+i\eta)]$	$\mathrm{Im}[\Gamma(002, 000; 0; \varepsilon+i\eta)]$	$\mathrm{Im}[\Gamma(022, 000; 0; \varepsilon+i\eta)]$	$\mathrm{Im}[\Gamma(222, 000; 0; \varepsilon+i\eta)]$
0.99	39.569079	−4.6817745	−6.2779541	−0.39049689
0.97	15.982229	0.50552364	−2.7438408	−1.7108800
0.95	10.162400	1.2551918	−1.4951536	−1.5158429
0.90	5.2354228	1.4688946	−0.27790187	−0.85055837
0.85	3.4173571	1.3463877	0.17521994	−0.39564724
0.80	2.4600328	1.1939637	0.38125359	−0.10079014
0.70	1.4632365	0.92026529	0.51134678	0.21193212
0.60	0.94861974	0.70047236	0.49414261	0.32446843
0.50	0.63486698	0.52293337	0.42341118	0.33530123
0.40	0.42398343	0.37717565	0.33355980	0.29297886
0.20	0.15914610	0.15486753	0.15065845	0.14651806
0.00	0.0	0.0	0.0	0.0

$$I=\mathcal{P}\int_0^a \frac{g(x)}{f(x)}\,dx+i\pi\,\frac{g(x_0)}{f'(x_0)} \qquad (\mathrm{A}\cdot 10\mathrm{a})$$

$$=\int_0^a \left\{\frac{g(x)}{f(x)}-\frac{g(x_0)}{(x-x_0)f'(x_0)}\right\}dx$$

$$+\frac{g(x_0)}{f'(x_0)}\cdot\log\left(\frac{a}{x_0}-1\right)+i\pi\frac{g(x_0)}{f'(x_0)}\,. \qquad \text{(A·10b)}$$

As the integrand in Eq. (A·10b) has been made regular at $x=x_0$, the integration may be performed straightforwardly.

Now, we calculate $\Gamma(j, j'; \delta; \varepsilon+i\eta)$, $\Gamma(j, l'; \delta; \varepsilon+i\eta)$, $\Gamma(l, j'; \delta; \varepsilon+i\eta)$ and $\Gamma(l, l'; \delta; \varepsilon+i\eta)$ for $1>|\varepsilon|>\sqrt{2\delta+\delta^2}/(1+\delta)$. We first change the integration variables from the Cartesian coordinates (x, y, z) to the spherical coordinates (r, θ, ϕ). We next integrate with respect to r and then with respect to θ and ϕ. If we consider the denominators of the integrands in Eqs. (A·1a, b, c, d) as functions of r, then they each have one single zero in the range of the integration. Thus we can use the method which was mentioned above to perform the integration with respect to r. The numerical integration was carried out on the NEAC 2200 electronic computer using Gauss' method with 28 points. We obtained the results for the several Green's functions for $\delta=0$ for 71 values of ε in the interval 0 to 1. Representative values are listed in Table II.*) Note that in this case the Green's functions are complex. The accuracy of the results is about 0.1% for the real parts, and it is much better for the imaginary parts. The results were used in the text to calculate the zero point contraction of spins.

Finally we consider the Green's functions at $\varepsilon=\pm\sqrt{2\delta+\delta^2}/(1+\delta)$. Here also it is convenient to use the spherical coordinates (r, θ, ϕ). Since the integrands of the expressions for the Green's functions do not diverge even at $r=0$, we can put $\eta=0$ beforehand and use the method of the direct numerical integration. The results for the several Green's functions for $\delta=0$ are also given in Table II. As before Gauss' method with 28 points was used in the calculation. We note that the value of $\Gamma(0, 0; 0; 0)$ coincides with Watson's value[8] of 1.3932 within the expected numerical error.

References

1) T. Wolfram and J. Callaway, Phys. Rev. **130** (1963), 2207.
2) S. Takeno, Prog. Theor. Phys. **30** (1963), 731.
3) Yin-Yuan Li and Yan-Qing Zhu, Acta Phys. Sinica **19** (1963), 753.
4) H. Ishii, J. Kanamori and T. Nakamura, Prog. Theor. Phys. **33** (1965), 795.
5) T. Tonegawa and J. Kanamori, Phys. Letters **21** (1966), 130.
6) T. Holstein and H. Primakoff, Phys. Rev. **58** (1940), 1908.
7) S. W. Lovesey, J. Phys. C (Proc. Phys. Soc.) [2] **1** (1968), 102, 118.
8) G. N. Watson, Quart. Appl. Math. **10** (1939), 266.
9) H. J. Guggenheim, M. T. Hutchings and B. D. Rainford, J. Appl. Phys. **39** (1968), 1120.
10) F. Keffer, Phys. Rev. **87** (1952), 608.

*) Readers desiring to know values for parameters other than those listed here should contact the author.

11) T. Tonegawa, to be published in Prog. Theor. Phys. Vol. 41, No. 1 (1969).
12) G. F. Koster and J. C. Slater, Phys. Rev. **95** (1954), 1167.
G. F. Koster, Phys. Rev. **95** (1954), 1436.
G. F. Koster and J. C. Slater, Phys. Rev. **96** (1954), 1208.
13) P. W. Anderson, Phys. Rev. **86** (1952), 694. Anderson considered only the case of $\delta=0$.
14) R. Kubo, Phys. Rev. **87** (1952), 568.
15) R. Kubo, Rev. Mod. Phys. **25** (1952), 344.